GEOLOGIC EVALUATION OF THE ETH MINING CLAIMS, EAST POTRILLO MOUNTAINS, DONA ANA CO., N.M.

by

David A. Jenkins

Submitted in Partial Fulfillment
of the Requirements for the Degree of
Master of Science in Geology

New Mexico Institute of Mining and Technology
Socorro, New Mexico

October, 1977

Abstract

The EPM mining claims were examined to determine if the potential for a silver deposit might be present. The claims are located along the northwest edge of the East Potrillo Mountains, in south-central New Mexico.

Four time-rock units crop out in the East Potrillo Mountains. These beds have undergone two periods of deformation; an early Laramide period of sharp anticlinal folding and associated thrusting and reverse faulting and a later period of Basin and Range type block faulting.

Mineralization, recrystallization and/or reconstitution on the EPM claims is confined to the Hueco Limestone. Jasperoid is the most prominent feature of reconstitution; it is located mainly along faults, fractures and breccia zones in two stratigraphic horizons.

Weathering and oxidation processes have greatly altered the surface expression of mineralization. Alteration minerals and high silver values (as high as 32.5 ppm) across the EPM claims indicate mineralization may have been locally developed. All evidence suggests that no major deposit is present; however, a small supergene or hypogene deposit of economic significance might be possible.

Table of Contents

Illustrations

List of Figures

List of Tables

List of Appendices

List of Plates

I. Introduction

Purpose

The EPH mining claims encompass several small ridges and knobs of silicified and mineralized rocks. Several earlier geochemical studies performed by William A. Bowes and Associates indicate high silver anomalies in the area. This investigation was undertaken to determine if the geology, structure and geochemistry of the area indicate possible ore zones below the surface, which might have economic potentials.

Location and Accessibility

The EPH mining claims are located in the south-central part of Dona Ana County, N.M. on the northwest edge of the East Potrillo Mountains. The claims are located in sections 3, 4, 5, 8, 9 and 10 of T.28 S., R.2W., approximately 30 miles west of El Paso, Texas and about 7 miles north of the U.S.-Mexican border (figure 1).

The claims can be reached from Interstate 10 in El Paso by exiting at Mesa Road and traveling 3 miles west to N.M. 273. One mile north along N.M. 273 a graded road is followed west parallel to the New Mexico-Mexico border through Strauss to Mt. Riley, an abandoned railroad siding. At Mt. Riley an unimproved road is followed northward for 7 miles to the EPH claims (figure 1).

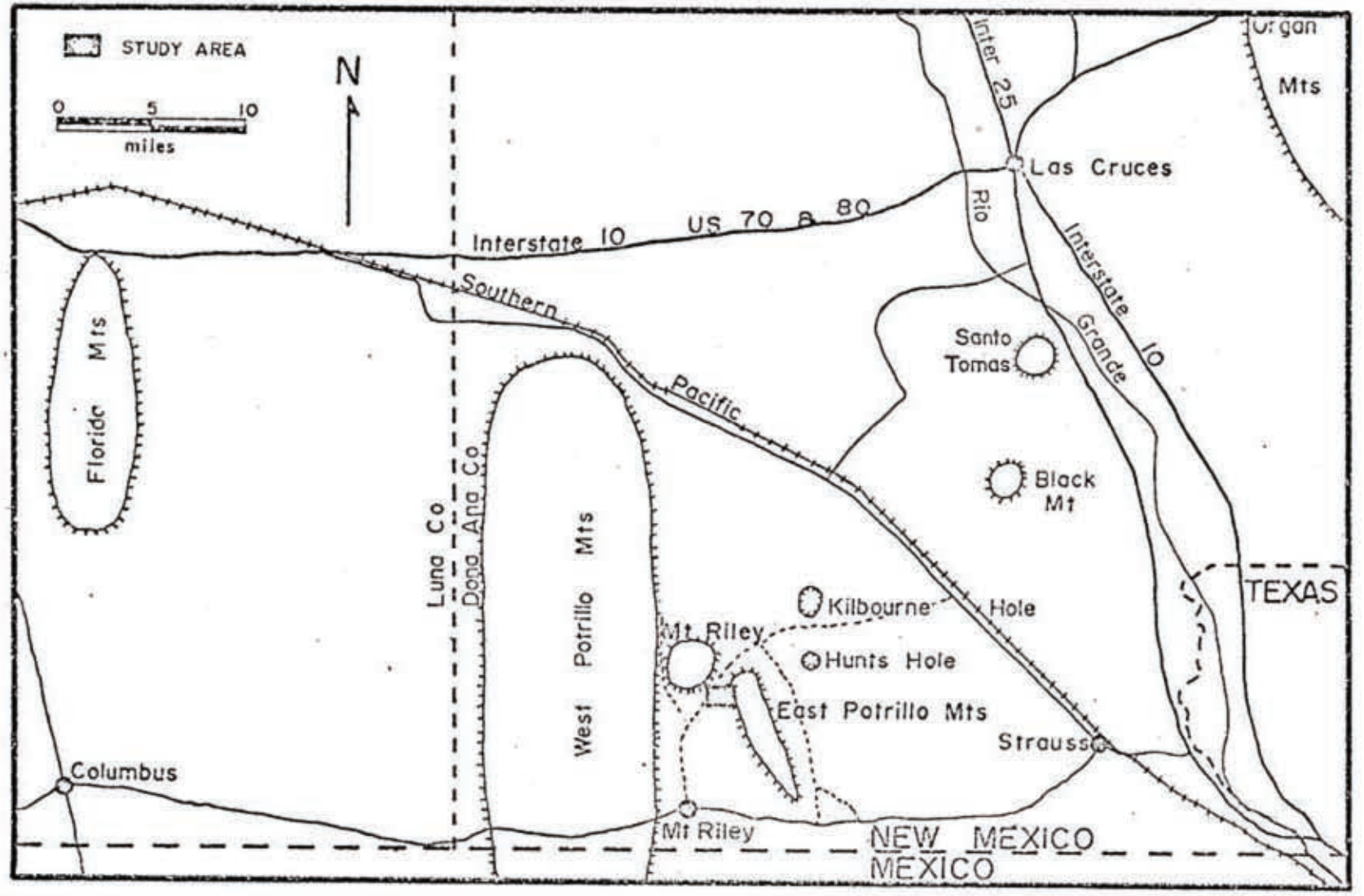

1.) Index map of south-central New Mexico.

Method

The original EPH mining claims, an area covering about 3 square miles, were mapped between August 1976 and May 1977 on a scale of 1:7585; the structure and geology of the area were determined and a sampling program designed.

Sampling was initially done at approximately 500 foot intervals with more detailed sampling in areas replaced by silica. A total of about 100 samples were collected. From these samples 92 thin sections were prepared and examined using a Zeiss Petrographic microscope. 92 samples were analysed for several elements which are indicators of mineralization in similar deposits. Analyses were done on a double beam Perkin-Elmer Model 303 atomic absorption unit.

Finally, 20 samples of barite and crystalline quartz were selected for study of their fluid inclusions. Homogenization temperatures of fluid inclusions were measured using a Bausch and Lomb petrographic microscope equiped with a homemade heating stage (Appendix A).

History of the EPH Mining Claims

The barite is thought to have been prospected around the turn of the century; however the EPH mining claims were first filed April 17-20, 1970 by J. Peter Rogowski, an employee of William A. Bowes. Barite prospects and jasperoid attracted Rogowski to the area. Samples were taken and claims filed based on the high silver anomalies

found. Originally 95 claims were filed but in 1975 the number of claims was reduced to 48 and refiled.

Previous Work

Detailed mapping of the East Potrillo Mountains was first done by Bowers (1960) as a master's thesis at the University of New Mexico. He reported the area to be made up mainly of Cretaceous units underlain by Permian rocks (figure 2). He interpreted the units to be faulted and folded into an asymetrical anticline.

An investigation of the Riley-Cox Pluton was conducted by Millican (1971) as a master's thesis at the University of Texas at El Paso. He concluded that the intrusion is an andesitic to rhyodacitic discordant structure.

Mengerd (1969) summarized the geologic history of southern New Mexico in a survey aimed at oil exploration, and the tectonic framework of southwestern New Mexico was examined by Corbitt and Woodward (1973).

Hoffer (1976) studied the Potrillo Basalt Field and gave a general summary of the geology of the East Potrillo Mountain area.

Preliminary sampling and analysis of the area was done by William A. Bowes and Associates during 1970 through 1975. Also during 1970 a program of shallow drilling in the area was carried out. The results of these surveys indicated high concentrations of silver in the area. In 1971 an induced polarization and resistivity survey was

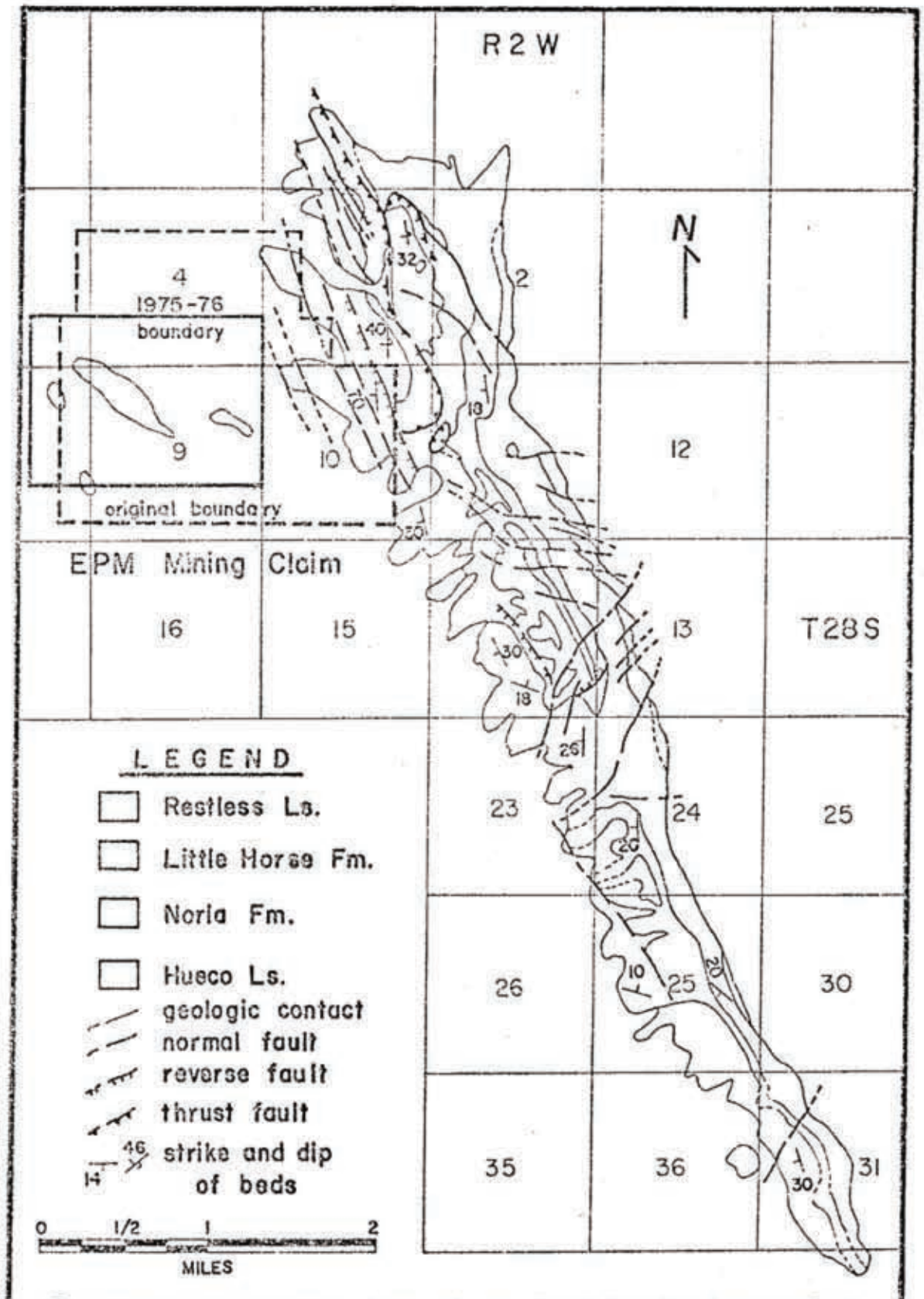

Generalized Geologic Map of the East Potrillo Mountains

adapted from Bowers, 1960

made across the claims. The survey was conducted by Phelps Dodge Corporation; they concluded that a faint dike-like feature is present under the area (Fink, 1972).

Acknowledgments

I wish to express my appreciation first to Dr. Clay Smith for his advice and comments on the many major and minor problems I encountered in the preparation of this thesis. I also wish to thank him for the long days he spent in the field with me.

I am especially indebted to Mr. William A. Bowes for his generous financial support throughout this study.

Marc Bodine and Antonius Budding provided helpful discussions and advice on many aspects of geochemical and structural problems.

Particular gratitude is due Lynn Brandvold of the New Mexico Bureau of Mines whose advice and help were essential to the annalysis of my samples. Michael Woolridge also with the Bureau of Mines is thanked for the fine job of drafting the accompanying map.

To my fellow students, Joe Iovenitti especially, thanks for the many discussions and valuable help given throughout this study. Bob Osburn is also thanked and praised for his fine drafting of the illustrations used in this report. Thanks is also extended to Katherine Deaderick who typed this paper.

I wish to thank also those peaple at the New Mexico

Bureau of Mines and at New Mexico Tech, who, too numerous to be mentioned specifically, nevertheless contributed to this study.

II. Geography and Physiography

Climate and Vegetation

The climate and vegetation of the East Potrillo Mountain area are typical of the Chihuahuan Desert. Over most of the studied area creosote bush is the dominant flora; ocotillo, yucca, mesquite, prickly pear and scattered junipers are also found.

Based on weather data from New Mexico State University at Las Cruces the average annual temperature for the East Potrillo Mountains is 60°F, with a monthly high averaging 80° for July and a monthly low average of 42° for January (Climatological Data, 1976). During the summer the days are typically hot and the nights cool. Winter months are characterized by mild days and cold nights. Precipitation in the area is generally between 8" to 10" annually, with most of this occuring in the summer months (USDA, 1972).

Topography and Relief

The East Potrillo Mountains are a northwesterly trending mountain range located on the western edge of the La Mesa surface. The La Mesa is a large plain that developed in the Mesilla bolson during mid-Pleistocene time (Hawley and Kottlowski, 1969). This plain extends from just north of Las Cruces southward into Mexico and is bounded on the west by the East Potrillo Mountains and on the east by the Franklin Mountains. The entire region is

included in the Mexican Highland section of the Basin and Range Province.

The East Potrillo Mountains rise over 1000 feet above the La Mesa surface. The highest point in the mountains is a peak reaching 5359 feet located just east of the EPM claims. The highest point, in the east central part, of the study area is at an elevation of 4950 feet, and the lowest spot in the southwest corner is 4300 feet above sea level.

To the northwest of the study area the peaks of Mt. Riley and Mt. Cox attain elevations of 5915 feet and 5957 feet above sea level respectively.

The EPM mining claims are characterized by several isolated ridges and hills of replaced limestone. These features stand in some places over 100 feet above the surrounding gently sloping landscape.

III. Stratigraphy

General

Four stratigraphic units have been recognized in the East Potrillo Mountains (Bowers, 1960); one Permian and three Cretaceous formations.

The Permian is represented by the Hueco Limestone. The Hueco is the only unit found within the detailed mapped area, and it is also the only unit that has been extensively replaced by silica.

Unconformably overlying the Hueco Limestone are three Cretaceous formations: lowermost is the Boria Formation overlain unconformably by the Little Horse Formation, which in turn is overlain disconformably by the Restless Limestone. These units were named and described by Bowers (1960) and were not studied in detail during this investigation.

Permian System

Within the mapped area the Hueco Limestone is generally medium gray in color, but in a few localities light gray and dark gray horizons can be found. The Hueco often weathers to a slightly lighter gray or tan.

The Hueco erodes in uniform slopes, except to the northeast of the study area where faulting has produced steep cliffs. Exposures are abundant, but complete sections are not available. The Hueco Limestone is usually well-bedded with layers ranging from 4" to 12" in thickness; however a

few beds attain a thickness of 18". In the western part of the study area the Hueco is more massive. The surface of the Hueco is usually quite jagged and rough with solution fretworks from 1/8" to 1/4" in height (figure 3).

Occasionally intraclastic beds of poorly sorted fragmented limestone less than two feet thick are found. The fragments are quite angular and are usually less than 6 inches in diameter (figure 4). These beds are quite distinctive as the fragments weather medium gray while the matrix weathers light gray or buff.

In the area studied the Hueco Limestone is consistently very fine grained. It has a whole rock density of about 2.69.

Most of the Hueco is not fossiliferous; however, the massive limestone along the southwestern side of ridge 9-1* is quite fossiliferous. No other exposures of this unit were found; gastropods and brachiopods make up approximately 5 percent of the rock (figure 3).

Two other units found in the lower part of the exposed section are included within the Hueco. These units have been completely silicified, so their original characteristics can only be estimated.

A small hill and knob (8-1 and 8-2) consist of quartzose siltstone. This unit is a very well-indurated light

* Prominent hills and ridges have been assigned coded numbers for easy reference, (see Plate 1).

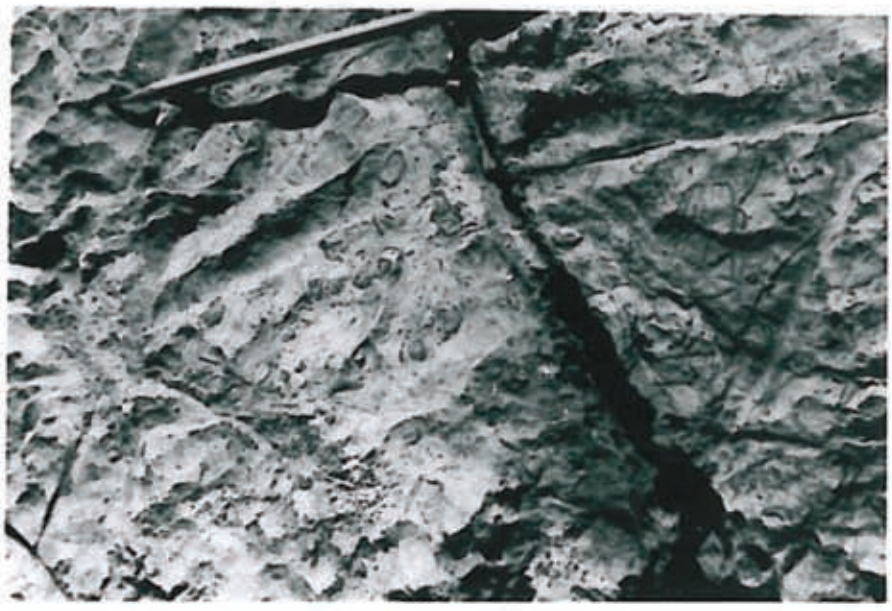

Figure 3. Fossiliferous limestone horizon, Brachiopods are clearly visible here. (location-station 94).

Figure 4. Intraclastic limestone horizon. (location-station 189).

gray siltstone with a grain size between 0.04 and 0.06 inches. Parts of the quartzose siltstone exhibit a faint relict bedding and in a few places cross-bedding can be found (figure 5). The very thin bedding, (0.1 inches), is marked by thin layers of dark material which are predominately iron and manganese oxides. Occasional vugs are present and are lined with quartz crystals. The vugs generally range from 0.5 inches to 3 inches in their largest dimension.

Figure 5. Truncated relict cross-bedding in quartzose siltstone horizon. (location--station 10)

The second unit included in the Hueco is a conglomerate located in the southwest corner of the study area (hill 8-3). The size of the clasts varies markedly: in some outcrops the largest clasts are up to 4 inches in diameter

whereas in others clasts a foot in diameter can be found. Most clasts are fairly well rounded and do not show any preferred alignment. Figure 6 illustrates the roundness and randomness exhibited by most clasts. Figure 7 shows a 5 inch clast which is different than most in this unit; it lacks rounding and exhibits relict bedding emphasizing the conglomeratic nature of the unit.

A complete measured section of the Hueco was not made due to silicification, faulting, and lack of outcrops, although the cross section (figure 15) indicates a minimum of 1245 feet of Hueco present.

Microscopically the Hueco is more than 90 percent micrite; sparry calcite usually makes up less than 10 percent of the rock, occurring in both veins and as vug fillings. Only one sample examined would be classified as sparry limestone and the sparry calcite in this sample appears to be the result of neomorphic recrystallization of micrite (neosparite).

Where the Hueco is fossiliferous the unit is a fossiliferous micrite (Folk, 1974), as the fossil content does not exceed 10 percent of the rock. Crinoids, brachiopods, and gastropods are present. Brachiopods are by far the most abundant fossil, usually making up more than 75 percent of the fossils. Slabbed sections of the fossiliferous beds indicate that the brachiopod shells were deposited in a random manner.

Pseudomorphs of hematite after pyrite are found in all

Figure 6. Silicified conglomerate horizon; note roundness and randomness of clasts. (location-about 30 feet west of station 205).

Figure 7. Clasts in silicified conglomerate horizon showing relict bedding. (location-about 30 feet west of station 205).

limestones except the neosparrite sample. The pyrite occurs disseminated throughout the limestone but concentrations are sometimes located along fractures and lining vugs. Detrital quartz is absent or occurs only in minor amounts.

The intraclastic horizons of the Hueco are also micritic. The clasts are angular and lack sphericity.

The quartzose siltstone horizons before silicification were made up of silt size (0.008 to 0.01 inches) quartz grains. The quartz grains are well rounded and spherical, and exhibit quartz overgrowths in optical continuity (figure 27). The original quartz grains which are present are well sorted.

In the quartzose siltstone horizon detrital chert grains are found in trace amounts. The thin layers that define the bedding in this unit are slightly enriched in oxides. Also, these beds have a matrix of very fine grained clays and silica. Quartz overgrowths are not as prominent in these layers.

Cretaceous Systems

Noria Formation

The Noria Formation is a light brown to gray sandy limestone. The base of the unit is a limestone pebble conglomerate grading upward into silty limestone and calcareous shale. Bowers (1960) measured three sections of the Noria Formation ranging from 270 feet to 602 feet in thickness. The two thinner sections are probably incomplete due to faulting.

Little Horse Formation

The base of the Little Horse Formation is a dark gray medium-grained limestone. It is massive to medium bedded. The upper part of the formation is a silty limestone which is locally fossiliferous. The Little Horse Formation weathers to a dull gray color. Three sections of the Little Horse Formation have been measured (Bowers, 1960); however only the thickest section (488 feet) is considered by this author to be complete.

Restless Limestone

The Restless Limestone is a massive fine-grained limestone at its base, grading upward into a silty and shaly limestone. The unit is medium gray in color. Only the thickest section of this unit is considered to be complete. The thickest section Bowers (1960) measured is 495 feet.

Correlation of Units

Bowers (1960) mapped and named the units in the East Potrillo Mountains, and his nomenclature is used in this study. However, it is desirable to correlate these units with surrounding areas, since the exposed stratigraphic column is limited.

The Franklin Mountains, Florida Mountains, Robledo Mountains and Big Hatchet Mountains are nearest to the East

Fotrillo Mountains and correlation with rocks in these ranges is likely to allow reasonable interpretation of stratigraphy (figure 8).

The oldest unit in the East Fotrillo Mountains was identified by Bowers (1960) as the Hueco Limestone from lithologic correlation to units in the Robledo and Franklin Mountains. From fossils collected, the unit is clearly Paleozoic in age (Kottlowski, 1977; Hook, 1977) but more precise dating is not available. This unit also represents the top of the Paleozoic section in the area. If it is the Hueco Limestone, its age is Permian, specifically Wolfcampian (early Permian).

The upper three units in the East Fotrillo Mountains were identified as Cretaceous by Bowers (1960) based upon fossil evidence. The Restless and Little Horse contain fossils of Fredericksburg age or older. The age of the Noria Formation was not determined, but Bowers observed that it resembled the basal Lower Cretaceous in southwestern New Mexico. He interpreted the Noria to be the same stratigraphic level as a red bed unit in the Big Hatchet Mountains (Zeller, 1953), and a conglomerate in southwestern New Mexico.

Craig (1972) studied the Cretaceous rocks in the East Fotrillo Mountains, and based on fossil evidence determined their ages to be Trinity with the possible exception of the Restless Formation which could be of Fredericksburg age.

In the Franklin Mountains both Cretaceous and Permian

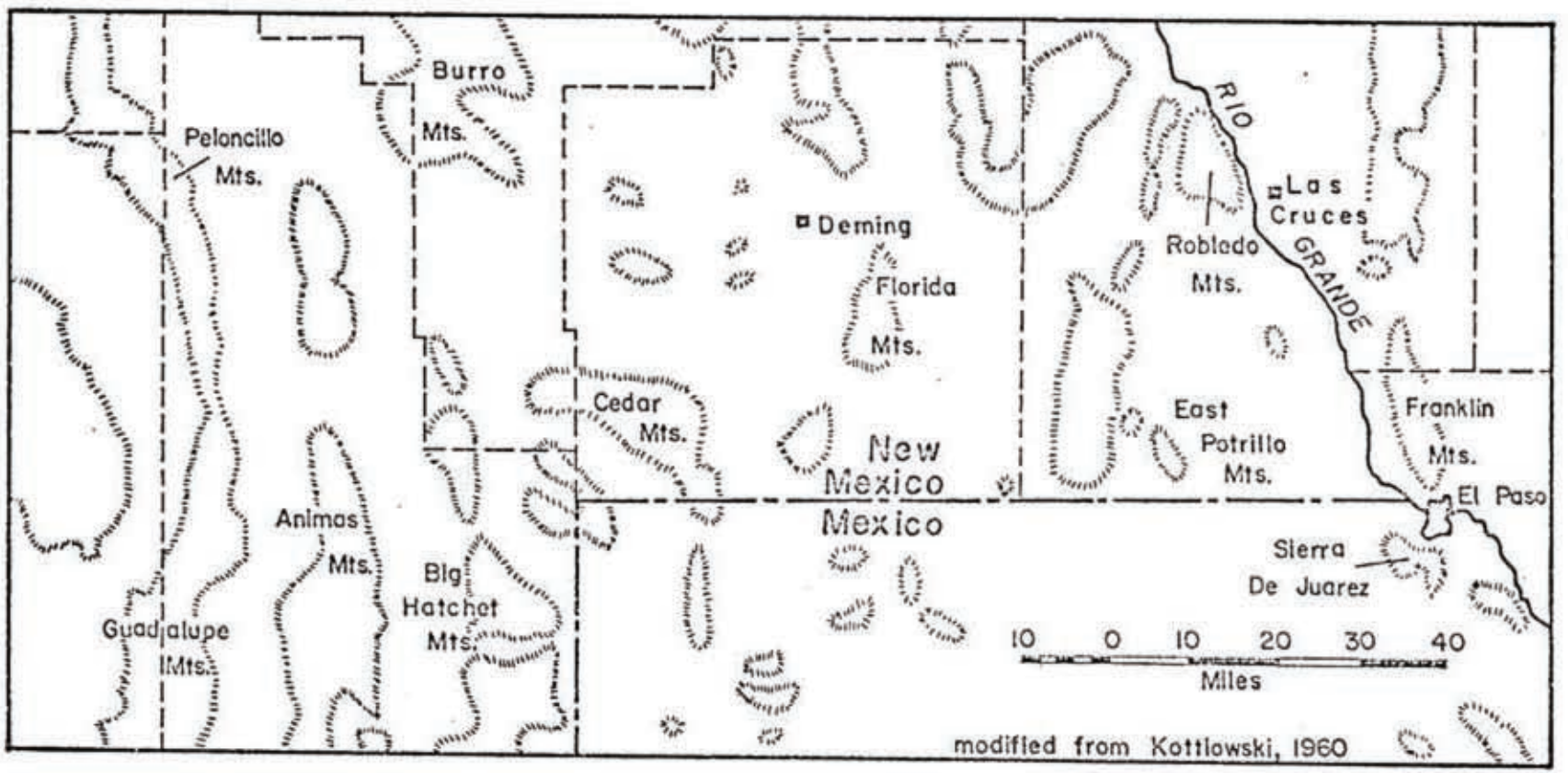

Figure 8. Index map of surrounding mountain ranges.

rocks can be found. The Paleozoic unit in the East Potrillo Mountains can be correlated with the Hueco cropping out there as was done by Bowers (1960). Harbour (1972) reported the occurrence of 2300± feet of Hueco Limestone in the Franklin Mountains where it is characterized by massive, gray, cherty, fossiliferous beds, and beds of marly yellowish siltstone. Fossils are present in the Hueco except for the middle of the formation. The Hueco in the Franklin Mountains as described by Harbour (1972) contains much more silt than in the East Potrillo Mountains.

The Cretaceous is poorly represented in the Franklin Mountains, but is presumed to lie directly above the Hueco. The Cretaceous in the Franklin Mountains probably correlates with the lower Cretaceous unit in the East Potrillo Mountains.

Correlation of rocks found in the East Potrillo Mountains with those in the Robledo Mountains is complicated by erosion; the Cretaceous rocks have been removed from the Robledo Mountains (Kottlowski, 1963). The Permian Hueco Limestone crops out in the Robledo Mountains however, and according to Bowers (1960) can be correlated, based on lithology, with the Hueco in the East Potrillo Mountains. In the Robledo Mountains there is about 1900 feet of Hueco present, including 190 feet of Bursum at the base and an Abo tongue about two-thirds of the way up in the unit (Kottlowski, 1963).

Both Cretaceous and Permian rocks can be found in the Florida Mountains. The Hueco of the East Potrillo Mountains

appears to be the same as the Hueco in the Florida Mountains as described by Corbitt (1971). Corbitt (1971) reported 548 feet of thin to massive, light to dark, fine to medium crystalline Hueco Limestone in the Florida Mountains. Shale beds were reported in the middle of the unit and the lower part was described as very fossiliferous, rich in gastropods, pelecypods and fusilinids (Corbitt, 1971).

Fifty to seventy-five feet of an unnamed silicified chert conglomerate of possible Lower Cretaceous age is found in the Florida Mountains (Corbitt, 1971). This is possibly equivalent to some part of the Noria Formation in the East Potrillo Mountains.

The Big Hatchet Mountains are located in southern Hidalgo County, New Mexico (figure 8). Although this range is not as close as the other ranges discussed above, it is included in this discussion because the geology has been worked out in considerable detail.

An almost complete Paleozoic section is exposed in the Big Hatchet Mountains. Only Silurian rocks are not represented. Also the units in this range are quite similar to those in the East Potrillo Mountains.

The Hueco Limestone is considered equivalent to Zeller's (1965) Horquilla Limestone. In the Big Hatchet Mountains Zeller (1965) measured 3245-3530 feet of Horquilla Limestone. The Horquilla in the Big Hatchet Mountains is characterized by medium-bedded bioclastic limestone in its lower third. The upper two-thirds are made up of basin,

reef and shelf facies rocks.

The Cretaceous of the East Potrillo Mountains is similar to the U-Bar and Hell-to-Finish Formations of the Big Hatchet Mountains. This indicates a considerable amount of erosion between the Permian and Cretaceous in the East Potrillo Mountains, as over 4000 feet of rocks in the Big Hatchet Mountains are missing in the East Potrillo Mountains (figure 9).

Figure 9 summarizes the nomenclature of the units in the East Potrillo Mountains and suggests relationships to those in the surrounding areas.

Cenozoic Era

The flat surface west of the East Potrillo Mountains and surrounding the silicified hills is covered with unconsolidated Holocene sediments. The sediments are chiefly fine grained, light brown sands. In some of the arroyos in the eastern part of the area coarser limestone fragments derived from the East Potrillo Mountains can be found. In the western part of the study area silicified limestone talus can be found surrounding the hills. The Holccene sediments are apparently quite thick as older rocks are not exposed in any of the arroyos except very near the base of the East Potrillo Mountains.

A wildcat oil well northeast of the East Potrillo Mountains on the La Mesa surface (sec. 32, T. 25 S., R. 1 E.) penetrated 12,800 feet of valley fill, volcanic rocks,

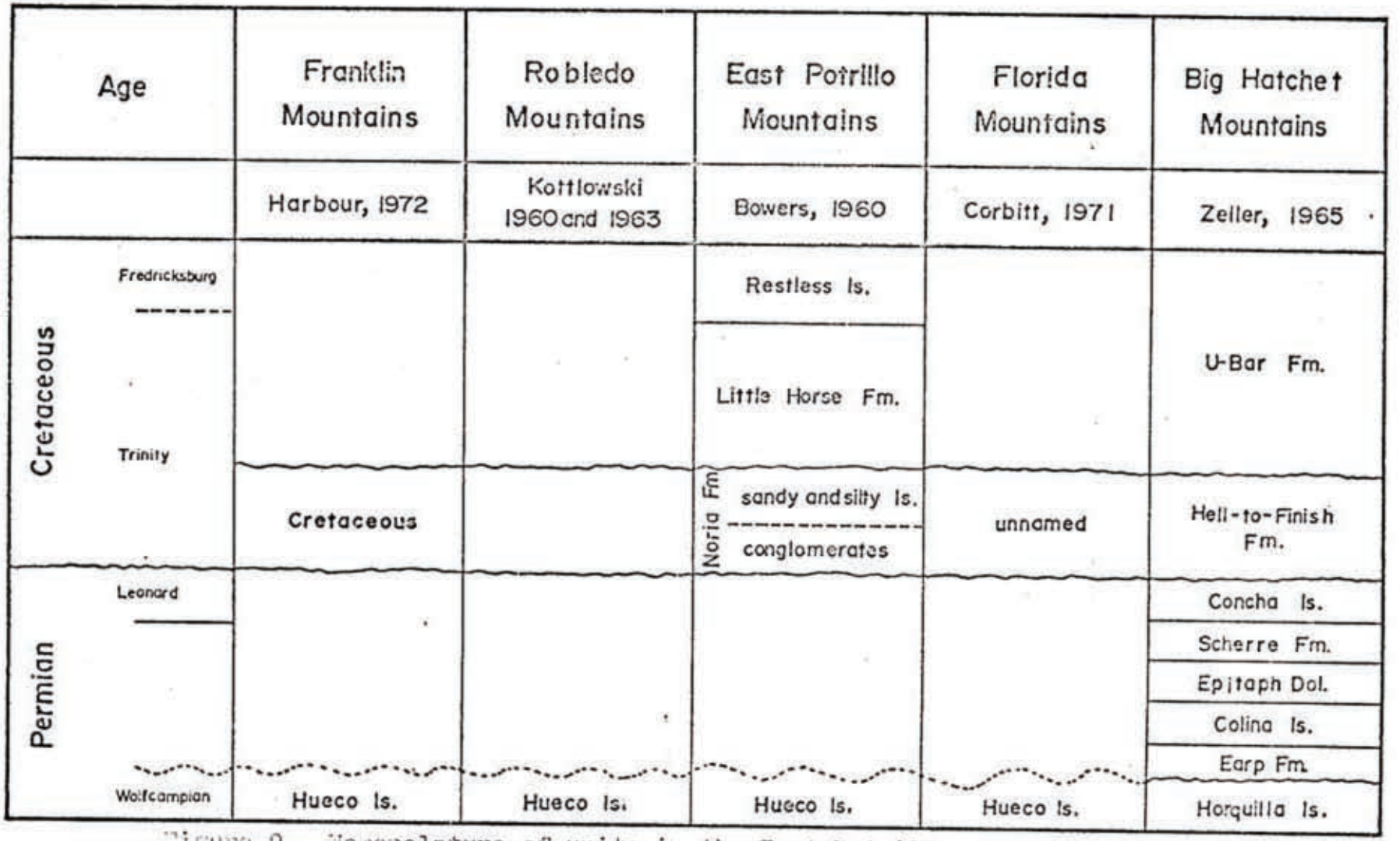

Figure 9. Nomenclature of units in the East Potrillo Mountains and surrounding areas.

Santa Fe Formation, sandstone and a coal unit all of Cenozoic age (Thompson and Bieberman, 1975).

Stratigraphic Column

The stratigraphic sequence is important for the interpretation of possible ore zones below the exposed Hueco Limestone. So far no deep drilling has been done on the EPM claims, so the proposed section may not be entirely correct. The underlying units have been extrapolated over large distances and the intrusion of the Mt. Riley-Mt. Cox pluton may have caused much disruption.

A proposed stratigraphic column of the East Potrillo Mountains is illustrated in figure 10. The Cretaceous section is a summary of the three thickest sections reported by Bowers (1960). The Permian section is a combination of work done by Bowers and this author. The pre-Permian part of the sequence is from a projected column of the Potrillo Shelf by Wengerd (1969).

It is possible that the Permian section is thicker than that presented, possibly up to 600 feet thicker.

Figure 10. Stratigraphic Column of the East Potrillo Mountain Area, Dona Ana Co., N.M.

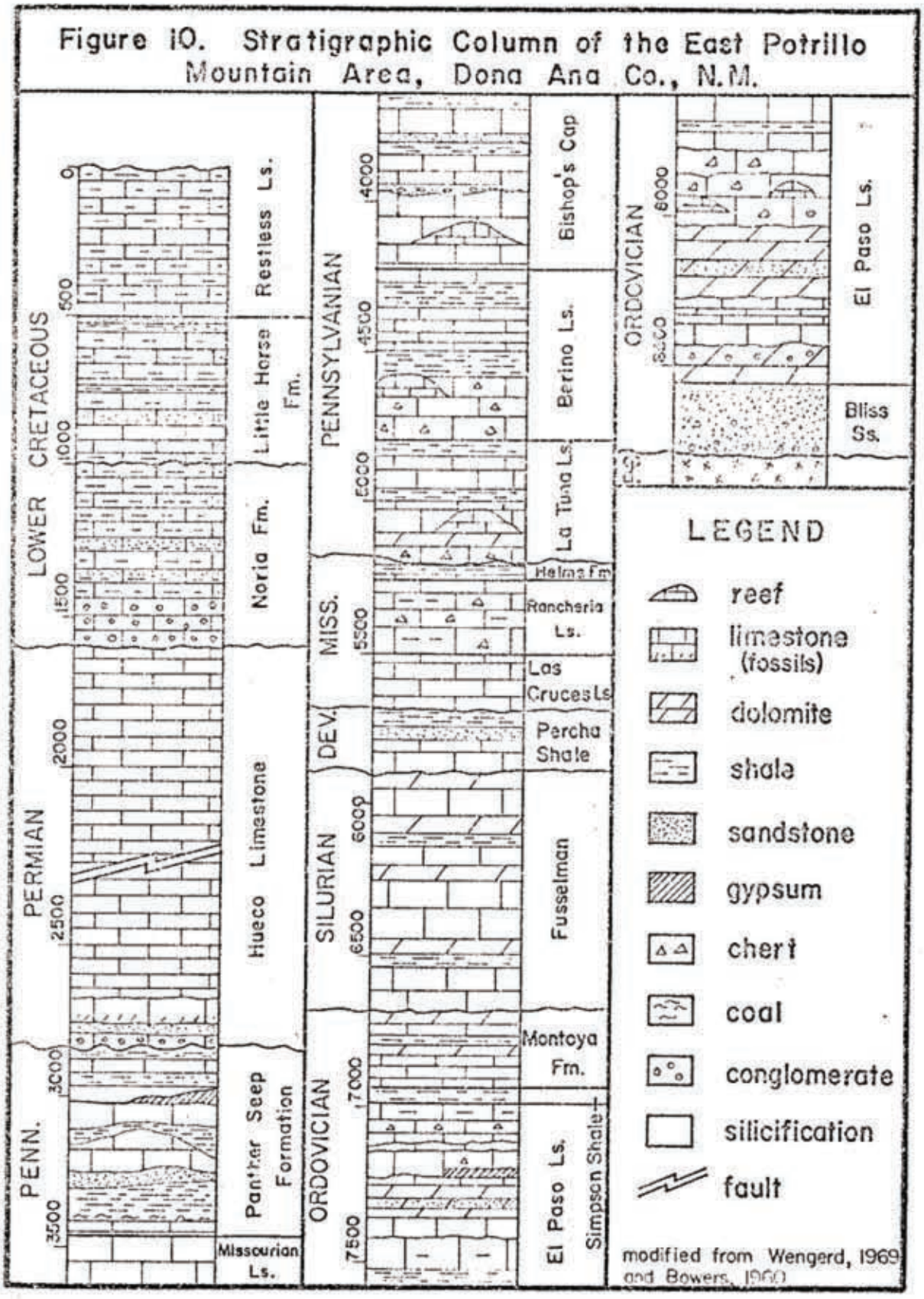

IV. Igneous Rocks

No igneous rocks are found in the study area, however both intrusive and extrusive rocks are found in the immediately surrounding area.

Intrusive Rocks

The major intrusive unit in the area is the Tertiary Riley-Cox pluton found to the northwest forming Mt. Riley and Mt. Cox (figure 1). The edge of the pluton is only about 1 mi. from the study area, and has a diameter of about 3 mi. The stock is a shallow intrusion that intruded Cretaceous and a sequence of Tertiary sediments and volcanic rocks (Millican, 1971).

The age of the Riley-Cox pluton is reported to be Eocene based on chemical and mineralogical similarities with the Campus Andesite, whose age was radiometrically determined (Millican, 1971). The Riley-Cox pluton appears to be a discordant structure of andesitic to rhyodacitic composition (Millican, 1971).

In the East Potrillo Mountains several nearly vertical dikes occur (Bowers, 1960). They generally trend northeasterly and cut all units. Millican (1971) felt that these dikes were probably related to the Riley-Cox pluton.

Two thin sections from the Riley-Cox pluton were examined. One sample is from the southeast side of Mt. Cox and the other from the southeast side of Mt. Riley

(Appendix D). Except for a slightly higher content of opaques and a lower degree of alteration in the Mt. Riley sample the two are virtually identical. The abundance of the various constituents in these samples was visually estimated as:

Plagioclase (An_{40})	- 62%
K-feldspar	- 16
Quartz	- 11
Biotite and Hornblende	- 9
Magnetite	- 2

making them rhyodacites.

In both samples the plagioclase is andesine as determined by the Michel-Levy method. The plagioclase laths are arranged in subparallel fashion, and are altered to kaolinite.

Extrusive Rocks

Extrusive rocks of Quaternary age are very abundant in the vicinity of the East Potrillo Mountains (figure 1). The West Potrillo Mountains are made up entirely of cinder and spatter cones and associated lava (Hoffer, 1969). These flows are known as the West Potrillo Basalts and are classified as alkaline olivine basalts (Renault, 1970). These basalts cover an area of more than 400 square miles, but average less than 20 feet in thickness (Hoffer, 1976).

There are two other areas of volcanic activity in the East Potrillo Mountain region, the Santo Tomas-Black

Mountain area, and the Aden Crater-Kilbourne Hole region (figure 1). Both of these areas are located on the east side of the East Potrillo Mountains. The Santo Tomas-Black Mountain flows are alkaline olivine basalts and are located along a chain of four eruptive centers. These flows are thought to be of Pleistocene age (Hoffer, 1969).

The other area of volcanism is a series of maar volcanoes, forming large depressions in the La Mesa surface. Kilbourne Hole, the largest of these maars, is over one mile in diameter and exceeds 300 feet in depth.

V. Structure

Setting

The East Potrillo Mountains are included within the Cordilleran foldbelt (Corbitt and Woodward, 1973). The Cordilleran foldbelt is bounded by the Peloncillo Mountains on the northwest and the Sierra de Juarez on the east (figure 8). This foldbelt is characterized by flat thrust faults, reverse faults and closely related overturned folds. Superimposed upon the foldbelt is Basin and Range block faulting.

Folds

For the most part, the bedding in the study area dips to the southwest. All of the beds are upright, except in the east-central part. The normality of the beds is indicated by truncated cross-beds (figure 5) found in the quartzose siltstone on hills 8-1 and 8-2.

The structure of the area is an overturned, anticlinal fold trending northwest. Overturned beds are found east of the study area, where Cretaceous beds (Noria) dip westerly underneath the Permian Hueco. This overturned contact is exposed on the small hill (3-1) to the northeast and along the crest of the range to the east of the study area.

In a few places folded beds are exposed over several hundred feet (figure 11). These subsidiary folds are

associated with larger anticlinal folding (figure 15); the smaller folds trend west-northwest and plunge about 10 to 20 degrees in the same direction. This orientation is approximately the same as that of the major anticline.

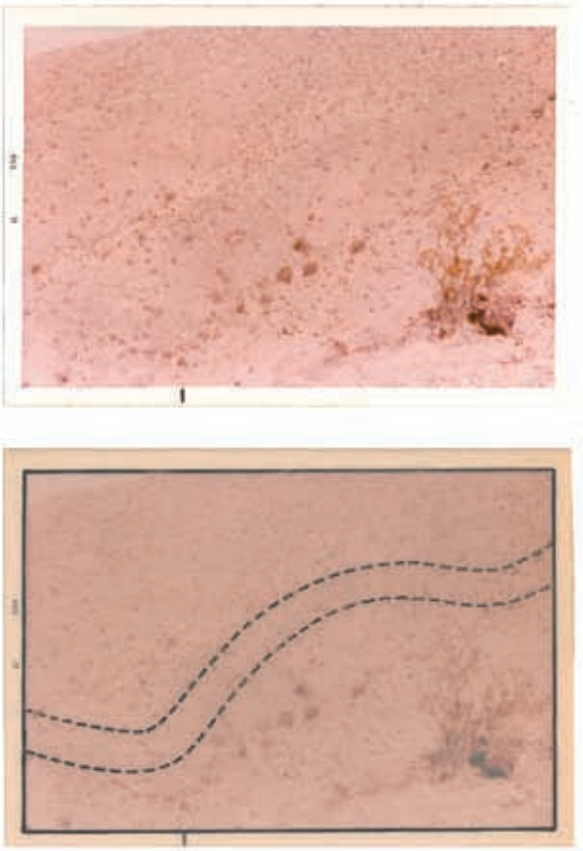

Figure 11. Small drag fold on the western limb of anticline. (location--about 1500 feet east of station 249)

Faults

The contact where the overturned and normal beds of the Hueco Limestone meet is not distinct and cannot be located readily in the field because of nearly parallel bedding on each side of the contact. From areal photo-

graphs the boundary can be located to the east of the field area. Bowers (1960) mapped this boundary as a reverse fault and this author agrees with his interpretation. The fault is associated with the folding and overturning.

Throughout the study area small faults are exposed, as illustrated in figure 12. The most common trend of these faults is to the northwest, with dips of 30-40 degrees to the southwest. These faults cannot be followed any great distance, and usually die out within 100 feet. Movement along these faults is generally only a few feet. Where movement direction could be determined normal faulting is indicated. It is along these small faults that silicification is most common. These faults are later than the folding and the thrusting, and even cut the igneous dikes in the area (Bowers, 1960).

Joints

In several locations within the silicified areas joint systems can be found. Individual joints generally extend less than 10 feet along strike. Some movement has taken place on these joints, since slickensides are sometimes observed (figure 13).

Structural Interpretations

The geologic structure of the EPM mining claims as presented below is basically the same as reported by Bowers (1960), except for two small changes. In agreement

Figure 12. Small normal fault surface (beneath hammer) dipping 30°SW with associated silicification. (location--station 151)

Figure 13. Slickensides on "joint" surface. (location--about 10 feet west of station 205)

with Bowers the area is the western limb of an overturned anticline (figure 14).

Bowers infers that the sediments in sections 1, 2, 8, and 9 of the study area are stratigraphically higher than those in sections 3 and 10. Although this is possible because of the lack of outcrops and stratigraphic control within the Hueco, this author believes them to be lower in the section (figure 15). The structural interpretation, as given in figure 15, is supported by several lines of evidence.

The most important evidence is the lack of any outcrops of the rock types found in sections 1, 2, 8, and 9 of the study area (conglomerate, quartzose siltstone and fossiliferous limestone) to the east. The absence of these units in the east does not indicate definitely that they are lower in the Hueco section. It is possible that they are missing because of thinning when the anticline was folded; however, the limestone beds in the east do not indicate that this type of deformation and thinning took place.

It is also possible that these beds were removed from the top of the unit by erosion; however, an unconformity with over 160 feet of relief over such a short distance is not easily envisioned. Another possibility that would allow the clastic beds to be higher in the section and still not be observed is to have part of the section removed by faulting (figure 14), which is the interpretation preferred by Bowers. Bowers' interpretation implies a thickness for the Hueco Limestone, which is much thicker than

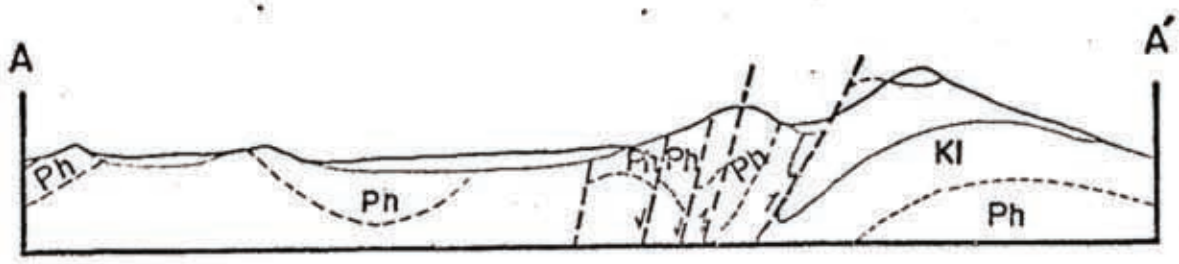

Figure 14. Generalized structural section through EPI mining claims and East Potrillo Mountains. (Appendix D) The Permian Hueco (Ph) and the Lower Cretaceous (Kl) units are shown. (modified from Bowers, 1960)

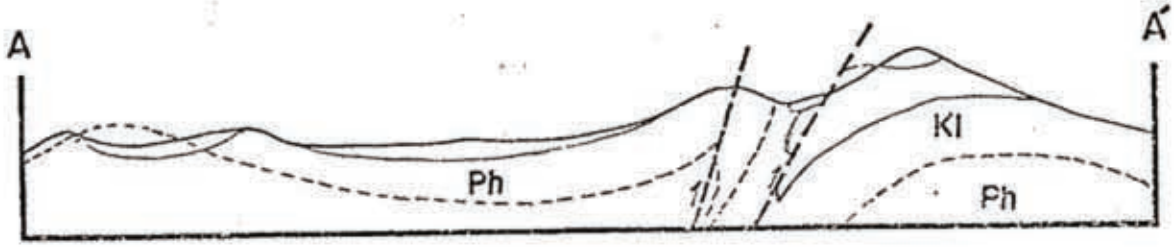

Figure 15. Proposed generalized structural section through the EPI mining claims and East Potrillo Mountains. (Appendix D) The Permian Hueco (Ph) and the Lower Cretaceous (Kl) are shown.

Kl Cretaceous

Ph Permian

Basal conglomerate of the Hueco Limestone

Note: Vertical scale is exagerated.

commonly accepted for the general area.

Other evidence that indicates that the clastic beds are lower in the section is the reinterpretation of the bedding attitude on hill 9-3. Bowers (1960) reports that the beds are dipping to the southwest while this author observed a northeasterly dip of about 40 degrees. Bedding was not measured directly on this hill as silicification was complete, but a foliation defined by vugs was measured (figure 16). The fact that vugs in silicified beds are often parallel to the original bedding can be seen along the south side of hill 10-1. In figure 17 it can be seen that vugs in the silicified beds do parallel the original bedding. In the Magdalena Mountains Loughlin and Koschmann (1942) also observed that the vugs in the silicified beds were parallel to the original bedding. Supporting the northeasterly dip is the geomorphic expression of hill 9-3; a steep southwest side and a gentle northeast side (figure 18).

Other supporting evidence of the low stratigraphic position of the conglomerate, quartzose siltstone and fossiliferous limestone beds are the lack of any significant clastic beds in the Hueco to the east. In the Florida Mountains (Corbitt, 1971), the lower Hueco is quite fossiliferous.

In figure 15, the reverse fault separating the upright beds of the Hueco from those overturned is shown to be steeply dipping to the southwest. It should be pointed

out that it may have been involved in the folding and shallow with depth. There is no evidence to indicate that the thrust does shallow with depth, and even if this is the case, it is still not likely that it comes close enough to the surface in the west part of the claim to affect the structure interpretation in figure 15.

Figure 16. Foliation interpreted as bedding on hill 9-3.

Figure 17. Limestone-silicified limestone contact showing parallelism of vugs in the silicified limestone with bedding in unreplaced limestone. (location--station 223)

Figure 18. Field area looking west from station 151. Note steep southwestern slopes and gentle northeastern slopes on hills in left middle ground (hills 9-1 and 9-3).

VI. Mineralization and Recrystallization

Introduction

The most prominent characteristic of the study area is the complete silicification of the Hueco beds in the western half. The original mineralization of the area is obscured by oxidation and weathering, as is the geochemical distribution of the metals examined in this study. The silicification most clearly represents jasperoid as defined by Lovering (1972):

> " an epigenetic siliceous replacement of a previously lithified host rock."

It is this jasperoid and high silver values found across the study area that make it a good target for exploration.

The replacement nature of the jasperoid is quite evident at the limestone-jasperoid contact on the south side of hill 10-1. Here the jasperoid can be seen to have moved up fractures and then moved out along some of the limestone beds (figures 19 and 20).

Occurrence

The effect that the joints and faults have in controlling the distribution of the jasperoid is quite apparent from the northwest trend of the silicified hills in the western part of the area. Major bodies of jasperoid are

only found within the Hueco Limestone, and are localized not only by joints and faults but also by stratigraphy. Stratigraphic control is best seen along the southwestern side of ridge 9-1; here the limestone has been completely replaced by silica, but just below this cap of jasperoid a fossiliferous horizon of unreplaced limestone can be found. This fossiliferous limestone can be traced discontinuously for over 1500 feet without any trace of replacement, while just 40 feet above is the jasperoid cap.

The size of the jasperoid bodies in the study area range from small pods only a few feet in length to composite masses extending thousands of feet.

Figure 19. Limestone-jasperoid contact showing fracture along which silica moved. (location--station 223)

Figure 20. Limestone-jasperoid contact showing jasperoid selectively replacing a limestone bed. (location--station 223)

Characteristics

The jasperoid of the ERH mining claims characteristically forms rugged outcrops, capping ridges and hill tops (figure 21). The extreme durability contributes to extensive jasperoid talus resulting in the impression that much more jasperoid is present than in actuality.

The color of the jasperoid is usually maroonish brown, gray or cream. Occasionally the original gray color of the host limestone is apparently retained. Weathered surfaces are most often rust brown in color but shades of yellow, orange, pink and red can be found. The color is

Figure 21. Jasperoid capping hill-top (8-3).

controlled mainly by the presence of iron oxides.

The texture of the jasperoids studied is quite varied. In all localities the jasperoid is aphanitic except for hills 8-1 and 8-2 in the western part of the claims, where the jasperoid has a sugary texture and the individual quartz grains are as large as 0.1 mm. In some outcrops the jasperoid is very uniform and massive, while at other localities it is brecciated into subangular clasts, and in a few localities breccia fragments can be seen to contain smaller breccia fragments. The clasts usually average less than 1 inch in diameter, however clasts as large as 5 inches in diameter are found (figure 22). In the Lake Valley District, New Mexico, Young and Lovering (1966) found textures in limestones near jasperoid bodies that indicate brecciation was prior to silicification. The

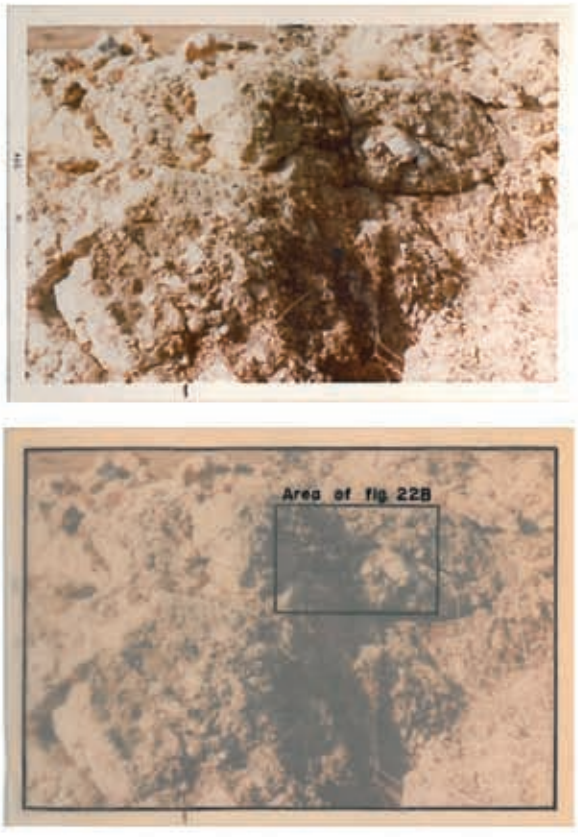

Figure 22A. Brecciated jasperoid, large clast in upper right is approximately 5 inches long. (location--about 50 feet east of station 85)

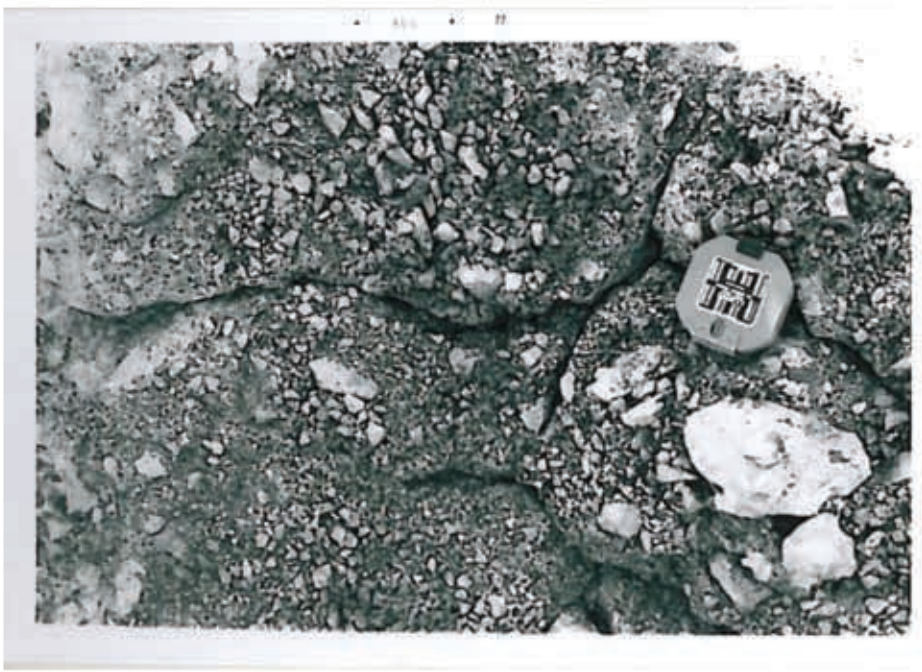

Figure 22B. Close-up view of above breccia.

specific gravity of the EPH jasperoids is between 2.54 and 2.57.

Vugs in the jasperoid are found throughout the mapped area but they are not very numerous and do not seem to be concentrated in any particular fashion. The size of the vugs found ranges from microscopic to a maximum of about 5 inches in length.

An interesting texture observed in two localities is ribbon rock (figure 23), consisting of alternating layers

Figure 23. Ribbon rock texture.
(location--station 209)

of crystalline quartz and jasperoid. The crystalline quartz has grown inward from the jasperoid toward the center of the crystalline quartz layers from both sides. The layers are generally less than 2 inches thick, averaging about 1 inch. These textures are more or less parallel to the original bedding.

The limestone-jasperoid contact is usually not exposed; however, in a few places the boundary can be seen. The contact on the south side of hill 10-1, where exposures are best developed, is very sharp (figures 19 and 20), with a transition from limestone to jasperoid requiring less than 0.05 mm. Gradational contacts extending over a 2 to 3 inches width can be found around some of the small (less than 10 feet in any dimension) patches of jasperoid.

Forty-four jasperoid samples were examined in thin section. These examinations were made to determine a paragenetic sequence, and to investigate the relations between microscopic characteristics and silver content. The textural terms used to describe the jasperoids are those proposed by Lovering (1970).

Several microscopic textures are observed in the EPM jasperoids, which include jigsaw-puzzle, xenomorphic, reticulated and granular. Usually within a given section one texture makes up essentially the whole specimen but occasionally a combination of two or more textures is found.

Lovering (1972) described a texture of highly irregular,

tightly interlocking quartz grains which resemble a jigsaw-puzzle. This texture is quite common throughout the EPI jasperoids. It is typically fine grained ranging from 0.005 mm to 0.15 mm, with most grains falling within the 10 to 30 micron size range. Jigsaw-puzzle texture often occurs in aphanitic homogeneous appearing jasperoids, and is found in eleven of the forty-four samples examined (figure 24).

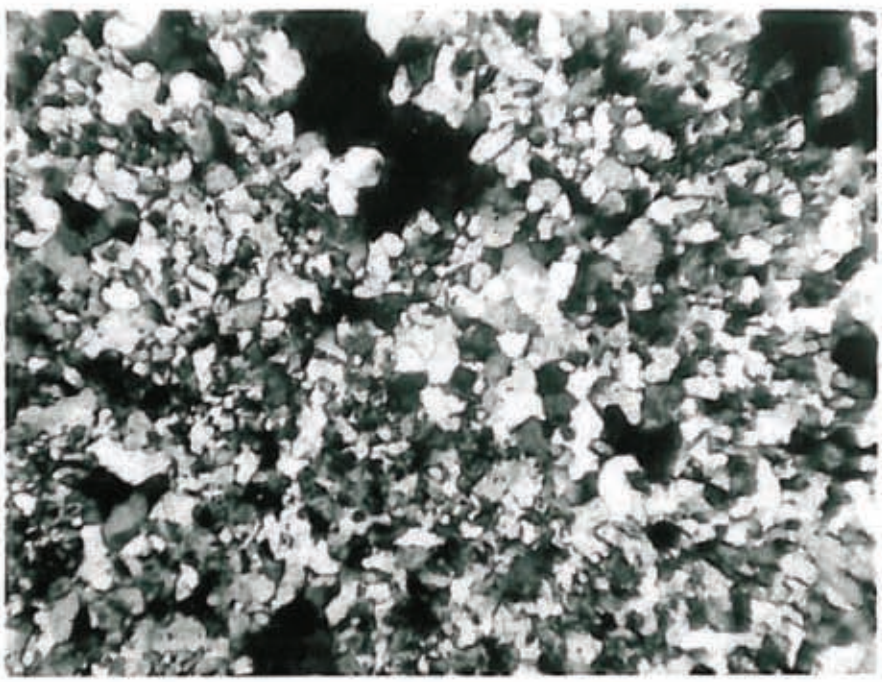

Figure 24. Jigsaw-puzzle texture. Field of view is 2.0 x 1.45 mm. (crossed nicols).

A second texture, quite similar to the xenomorphic texture commonly observed in igneous rocks, is equally represented across the EPI claims. Xenomorphic texture is composed of irregular anhedral grains of quartz, quite

similar to jigsaw-puzzle texture except lacking the more amoeba-like contacts. Grains range in size from 0.015 to 0.3 mm with an average of about 0.05 mm (see figure 25).

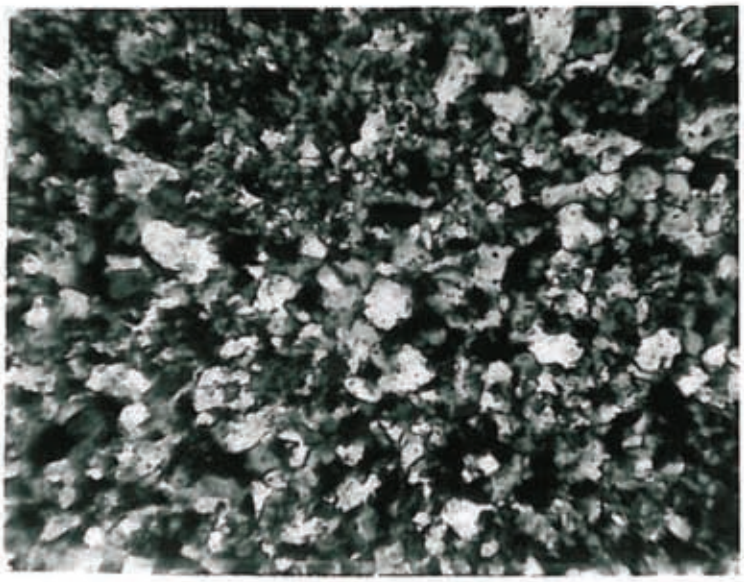

Figure 25. Xenomorphic texture. Field of view is 2.0 x 1.45 mm. (crossed nicols).

Reticulated texture (figure 26), also found in eleven of the forty-four samples studied, is characterized by elongated grains with a length-to-width ratio of 3:1 or greater. Lovering (1972) found this texture to be useful in separating jasperoids from other siliceous rocks such as cherts or novaculite as this texture is restricted to jasperoids.

Two other textures observed are combinations of jigsaw-puzzle-reticulated and jigsaw-puzzle-xenomorphic, occuring in 2 and 5 samples respectively.

Figure 26. Reticulated texture. Field of view is 2.0 x 1.45 mm. (crossed nicols).

A granular texture is found in the quartzose siltstone horizon. This rock type may not be considered by some to be a jasperoid, because it is not the result of the replacement of one rock type by another. Much of the unit (approximately 80%) was initially quartz grains, and only about 15 to 20% of the rock is the result of siliceous replacement, forming quartz overgrowths in optical continuity with the original quartz grains, as illustrated in figure 27.

A brecciated structure can often be seen in thin section. Subangular to angular fragments are much more evident in plane light than under crossed nicols. In plane light the breccia fragments are finer grained than the matrix, but the reverse is sometimes found.

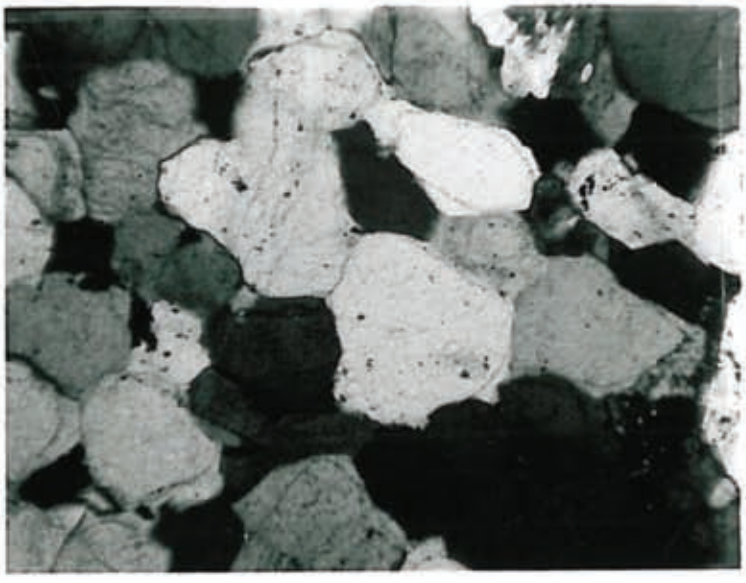

Figure 27. Granular texture showing quartz overgrowths. Field of view is 2.0 x 1.45 mm. (crossed nicols).

Vugs are commonly seen in some of the samples, and are often lined with quartz crystals. The quartz crystals are stressed and give a biaxial figure even in vugs that have not grown completely closed. Vugs near the limestone-jasperoid contact sometimes have calcite coating the quartz crystals or even completely filling the centers.

In thin section the limestone-jasperoid contact is a zone of pure microcrystalline jasperoid with a sharp transition to a zone of finer grained jasperoid and limestone, which grades into pure limestone. Figure 28 is a microphotograph of a contact.

The thin section study also revealed iron oxides in many of the jasperoids. These are represented mainly by

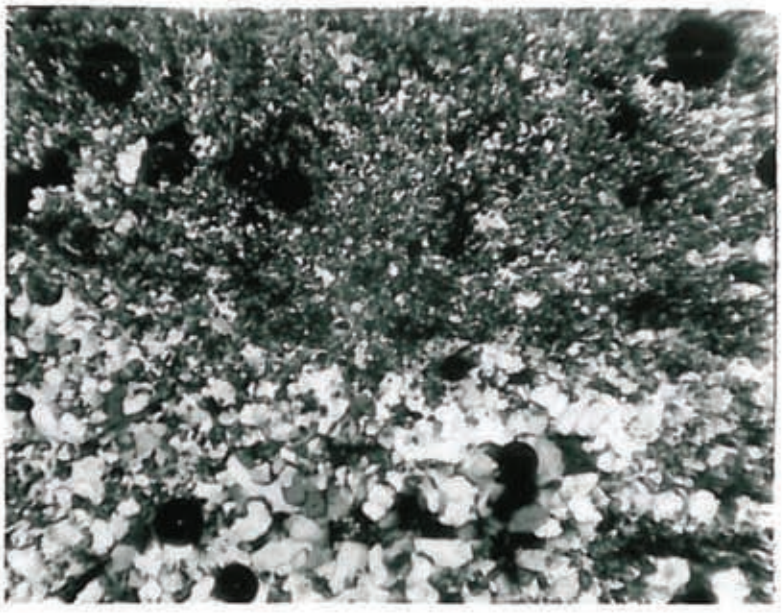

Figure 28. Microphotograph of limestone-jasperoid contact. Dark area in upper half of photo is limestone, and lighter crystalline lower half is jasperoid. Small light grains in limestone are quartz. Field of view is 2.0 x 1.45 mm. (crossed nicols).

pseudomorphs of hematite after pyrite. Usually the oxides account for less than 1% of the sample, however in one sample hematite amounted to about 7%. Limonite is found as a final coating in fractures of a few samples.

In about one-forth of the jasperoid samples barite is found. It occurs as a late stage mineral found in vugs or at the center of veins. Figure 29 shows barite crystals which have grown at the center of a vein.

Also, calcite is found in most of the jasperoids. It occurs as very small (@0.01mm) specks throughout the rock. In samples that exhibit reticulated texture, calcite inclu-

Figure 29. Barite growing in center of vein on crystalline quartz, which in turn is growing on microcrystalline quartz. Field of view is 2.0 x 1.45 mm. (crossed nicols).

sions are often found in the center of elongated grains (figure 26). Recrystallized calcite is sometimes found near the limestone-jasperoid contacts, where it partially fills the center of vugs.

Several samples collected from five prospect pits in the area were studied. These prospect pits are commonly small, as are the bodies of mineralization on which they are located and they usually delineate faults or shear zones of limited extent.

The prospect pit on hill 10-1 is unique in its mineralization. This pit was dug on an exposure of jarosite, probably potassium jarosite, $K_2Fe(OH)_{12}(SO_4)_4$.

The jarosite at this locality is an oxidation product of goethite and hematite, which can be found around the hill to the south of the pit. A similar swirling texture in the three minerals as well as jarosite associated with the goethite and hematite in sample 202A substantiates the close relationship.

Four prospect pits were examined which are located on barite mineralization. One prospect pit is located along the east edge of the EPM claims (station 172); another is located in the northeast corner of the claims (station 100); a third is northeast of the claims on hill 3-1 (station 230 L) and the fourth is about one mile north of the claims in section 34 along the crest of the East Potrillo Mountains (station PP).

Traces of malachite staining can be found at all of the barite prospects, however a significant amount of staining is found only at prospect pit PP. Galena is found in all of these barite bodies, and surrounding the galena in all cases are rims of cerrussite (figure 30). Calcite is found at all of the prospect pits and at station 100 dolomite was also identified. Pyrite altering to hematite is found in the jasperoid portion of the samples from prospect pits 172 and 100.

Paragenetic Sequence

A generalized paragenetic sequence has been developed for the mineralization and recrystallization of the EPM

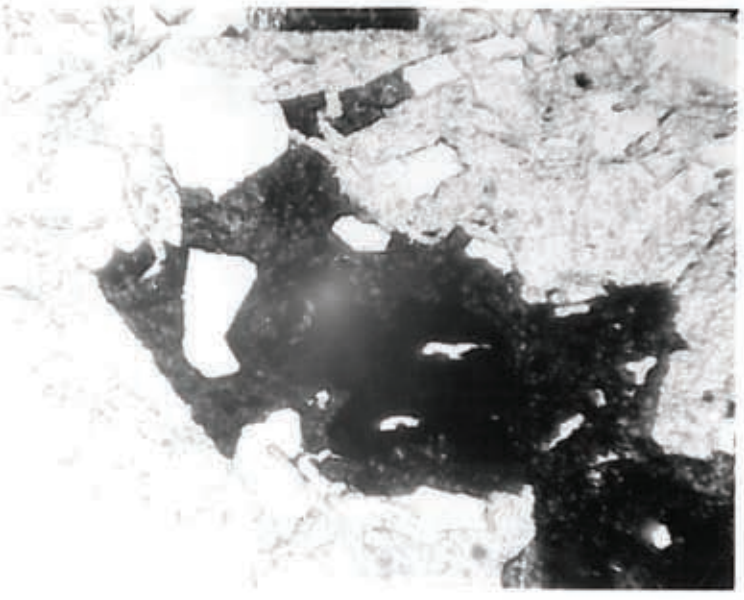

Figure 30. Galena (solid black) altering to cerrussite (mottles black). Field of view is 2.0 x 1.45 mm. (uncrossed nicols).

claims. The paragenetic sequence shown in figure 31 illustrates the relative times of deposition, not the amounts of material deposited. The microcrystalline quartz (jasperoid) may not have been continuously deposited as shown in figure 31, but may have been introduced in pulses or just in varying amounts. Non-continuous deposition is indicated by the different textures that are sometimes observed in a single sample, and the silicified breccias.

Fluid Inclusions

The initial objectives of the fluid inclusion study were to determine 1.) the temperature of mineralization associated with the jasperoid and 2.) if there is any areal

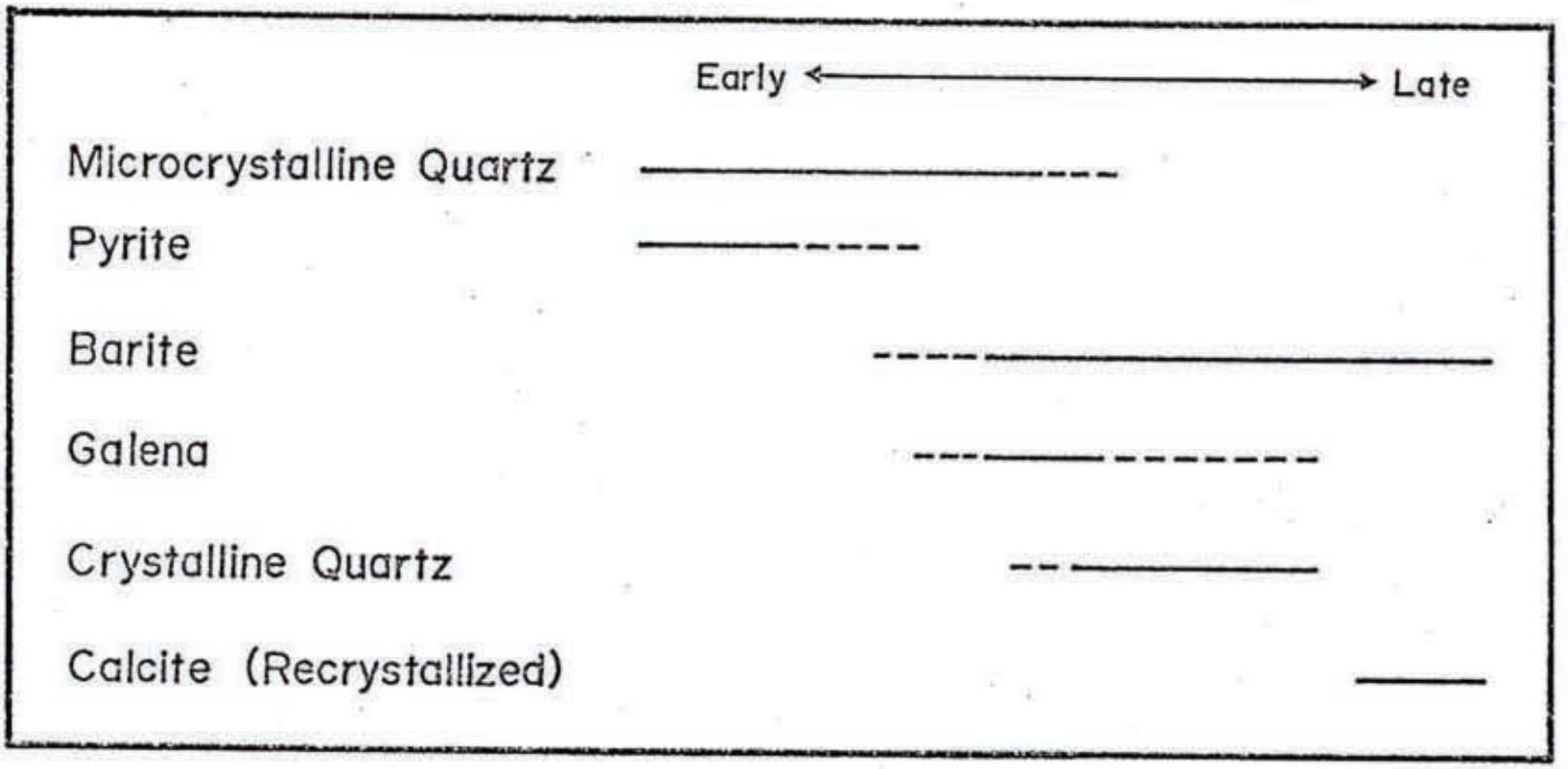

Figure 31. Paragenetic sequence for the mineralization and recrystallization of the [illegible] mining claims.

distribution of homogenization temperatures, which might indicate the direction of fluid movement.

Twenty samples of barite and crystalline quartz were collected and prepared for fluid inclusion study. Ten of the samples, 7 barite and 3 quartz, did not contain suitable inclusions for study. The microcrystalline quartz was not studied for fluid inclusions because of its extremely fine grain size, and lack of suitable inclusions.

The quartz samples were collected from vugs except sample 209 which is from a crystalline layer of ribbon rock. The size of the inclusions studied ranged from about 0.02 to about 0.12 mm with most approximately 1/30 mm in diameter. The inclusions studied are considered pseudo-secondary as their primary nature could not be proven. All of the inclusions studied were simple two phase inclusions of gas and liquid.

Four of the samples which contained inclusions did not yield satisfactory results. Their temperatures are considered unreliable because of large ranges in the homogenization temperature, or only one inclusion could be found.

The inclusion filling temperature data is listed in Table 1; the pressure corrected temperature, the average filling temperature, the range of filling temperatures, and the number of inclusions measured are shown. The locations of the samples from which fluid inclusion temperatures were measured are shown on Plate 1. The temperature of sample F1-4 is given as a range because some of the lower temp-

eratures measured may not be correct since they were measured on very small inclusions.

An approximate pressure correction was made on the homogenization temperatures. The maximum overburden on the Hueco could not have been more than the total of 16,000 feet of post-Hueco units. This amounts to a little less than 5 km. At 250 degrees the temperature correction for this overburden is only 70°C. The mineralization seems to be of Tertiary age however, which makes a maximum overburden of only about 6000 feet much more likely. With this lower pressure (approximately 500 bars) correction, ΔT for increased pressure is less than 40°C (Ingerson, 1947).

The range of homogenization temperatures measured indicates that replacement was done at hydrothermal temperatures. Unfortunately the number of suitable inclusions measured was small and no areal temperature gradient can be seen.

Freezing temperatures to determine the salinity were not done. Hall and Friedman (1963) reported a salinity of about 9.3% for quartz of the Cave-in-Rock fluorite district in Illinois. Na and K were the major cations and Cl was the major anion. Lovering (1972) believed that Hall and Friedman's reported salinity was a good estimate of those from which ore-related jasperoids are deposited. Correcting the homogenization temperatures for pressure makes the actual temperature of crystalline quartz deposition approximately 195-238°C.

Sample	Number of Inclusions Measured	Range of Filling Temperatures	Average Temperature °C.	Corrected Temperature °C.
F1-2	4	155-207	189	214
F1-3	3	190-197	192	220
F1-4	7	127-180	152-180	185-208
F1-6	6	158-240	212	238
F1-8	2	155-160	158	195
209	8	179-193	184	210

Table 1. Results of fluid inclusion study.

Geochemistry

A geochemical survey of five elements was made across the EPM mining claims. Ninety-two samples were analysed by standard atomic absorption techniques. A variety of rock types were analysed in the hope of finding where the silver is concentrated.

Because of the large number of samples that were analysed, all of the samples were not done in duplicate, however, fourteen samples were repeated and a reproducibility of about 7 percent can be expected for all the elements. Eight samples were commercially analysed by William A. Bowes and Associates of Steamboat Springs, Colorado. Analyses were done by emission spectroscopy, a semiquantative technique and good agreement with my results is found.

The choice of elements studied was based on analyses made earlier by W.A. Bowes and Assoc. Silver was naturally studied as it is the target metal of the EPM claims. Copper and lead were examined as the earlier results showed large fluctuations in their concentration; it was hoped that they would give an indication of mineralization intensity. Calcium and magnesium were studied with the intent of identifying stratigraphic zones.

Silver

Silver is the metal that is of direct interest to this study. Silver is very often associated with or near jasperoid bodies. Some examples are the Taylor Mining

District near Ely, Nevada (Lovering and Heyl, 1974), Leadville District, Colorado (Lovering, 1972), Tintic District in Utah (Lovering, 1972), and the Eureka District of Nevada (Lovering, 1972).

Goldschmidt (1954) estimated the average lithospheric content of silver to be about 0.02 ppm. The average concentration of silver in carbonates is approximately 0.04 ppm (Turekian and Wedepohl, 1961), and Lovering (1972) found the median silver concentration in jasperoids to be about 1 ppm.

The large univalent silver ion enables easy leaching and transport by surface waters, where it is usually transported as the sulfate (Rankama and Sahama, 1950). Silver can be reprecipated below groundwater level, often in carbonate rocks. Secondary silver often occurs as the metal, antimonides, and sulphosalts, or in galena. Generally in the oxidation zone silver is quite mobile (Naumov et. al., 1969). However, in arid regions silver is not excessively mobile and cerargyrite (AgCl) is often formed in the oxidation zone (Dunham, 1935; Young and Lovering, 1966).

Copper

Lovering (1972) reported the median copper concentration of 200 jasperoids to be about 30 ppm. The average concentration of copper in carbonates has been reported to be about 4 ppm (Turekian and Wedepohl, 1961). The most important primary copper mineral is chalcopyrite. Copper also can be leached and reprecipitated much the same way as silver. Copper is also often transported as the sulfate

and redeposited as the carbonate (Rankama and Sahama, 1950). In the oxidation zone copper has the highest mobility as compared to silver and lead (Naumov et. al., 1969).

Lead

Lead in jasperoid has a median concentration of about 20 ppm (Lovering, 1972). Turekian and Wedpohl (1961) reported the average composition of the lead in carbonates as 9 ppm. In the zone of oxidation lead has the least mobility of the elements silver, copper and lead, because of alteration of PbS to the relatively stable minerals cerrussite and/or anglesite.

Results and Interpretations

The analyses made by this author and those done commercially are listed in Appendices B and C. The Fe, Cr, Ni and possibly the Mn results of the commercially analysed samples are not accurate, and are due to contamination as a result of sample preparation. The location of sample sites is shown on Plate 1 and in Appendix D.

The five elements analysed (Ag, Cu, Pb, Ca, Mg), Ca/Mg ratios, modal opaques, barite, vugginess, crystalline quartz, brecciation, color (darkness), and texture were evaluated and their coefficients of linear correlation determined. Color and texture were assigned ordinal and nominal scales; color was assigned values of 1-3 going from dark to light, and texture was assigned values as follows; jigsaw-puzzle-1, xenomorphic-2, reticulated-3, and

granular-4. Because these are not interval scales, correlation coefficients of the variables may be suspect. The correlation coefficients of the variables indicate that none of these variables are related to each other, at least linearly.

The geochemical similarities and differences of the jasperoids and limestones are compared in figures 32, 33, and 34; these figures are plots of Ag versus Cu, Pb and Ca/Mg. Some interesting generalizations can be made from these graphs. The graph Ag versus Cu (figure 32) shows the average Ag content of the jasperoids and the limestones to be essentially the same. Figure 32 also shows that although low, the Cu content of the jasperoid is significantly higher than that of the limestone. The final feature that should be noted about this graph is the fact that the Ag and Cu concentrations of the jasperoids are much more widely dispersed than in the limestones.

Figure 33 shows Ag concentration versus Pb. The Pb values for the majority of limestones are grouped over a small area. The Pb concentrations in the jasperoids are both higher and lower than that of the limestone.

Figure 34 shows Ag content versus the Ca/Mg ratio. The Ca/Mg ratios of the limestones occur in two groups. One group of ratios lies at or less than 4 and the other is found above 70. The Ca/Mg ratios for tha jasperoids are located between these two groups.

Several miscellaneous samples were also analysed. As

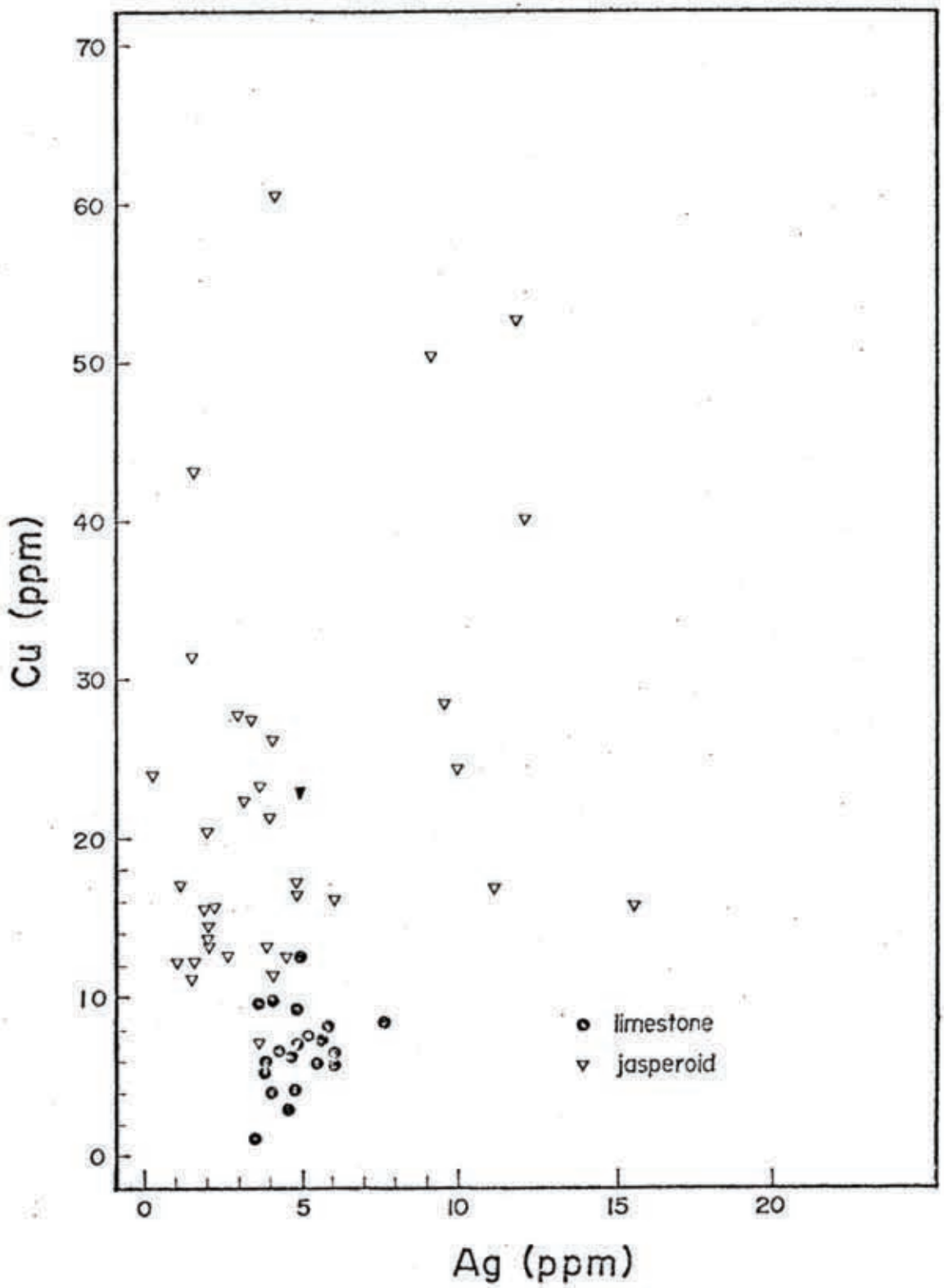

Figure 32. Graph showing relationship of copper concentration to silver in limestones and jasperoids. ▾ average jasperoid concentration. o average limestone concentration.

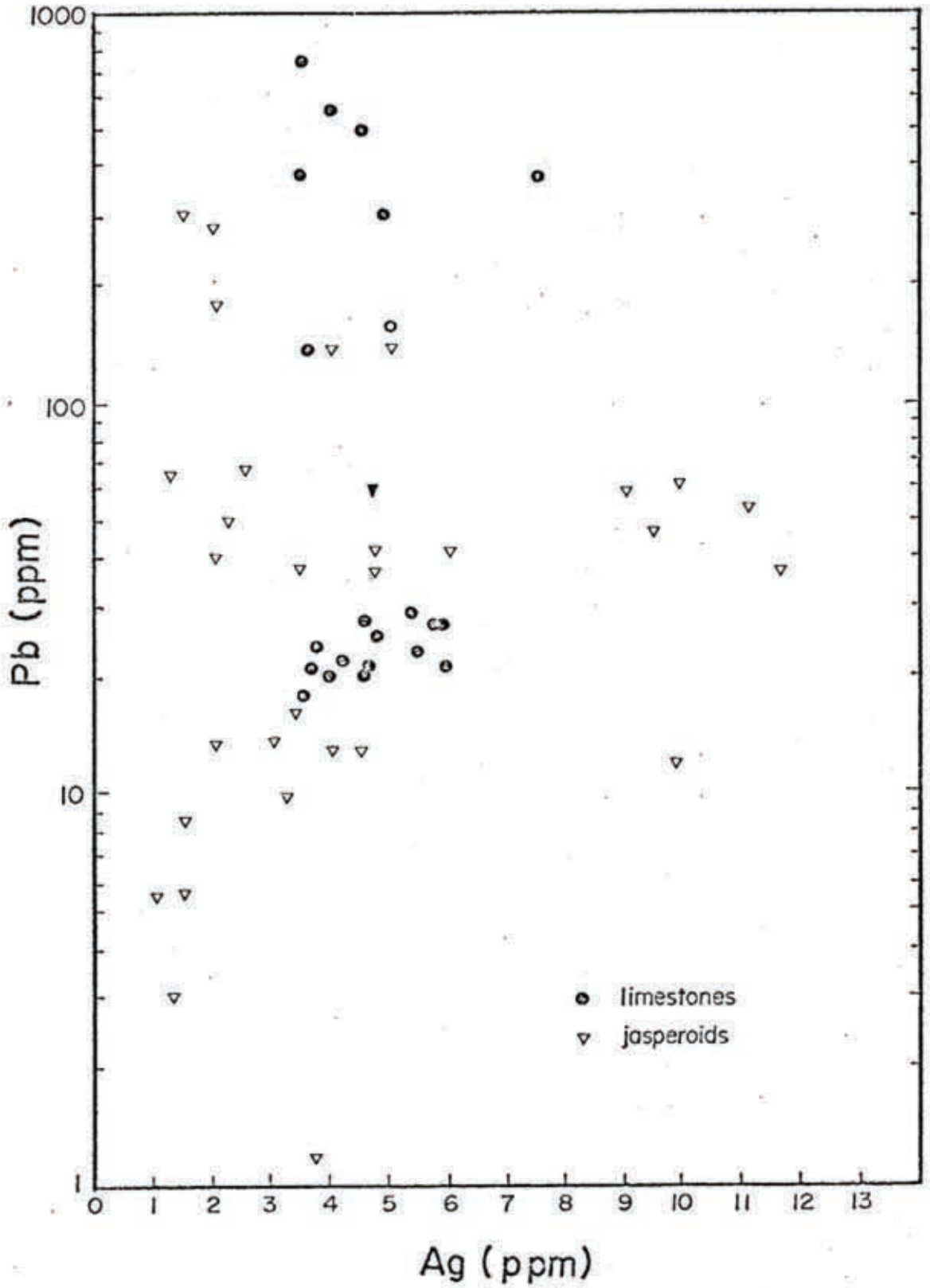

Figure 33. Graph showing relationship of lead concentration to silver concentration in limestones and jasperoids. ▾ average jasperoid concentration. o average limestone concentration.

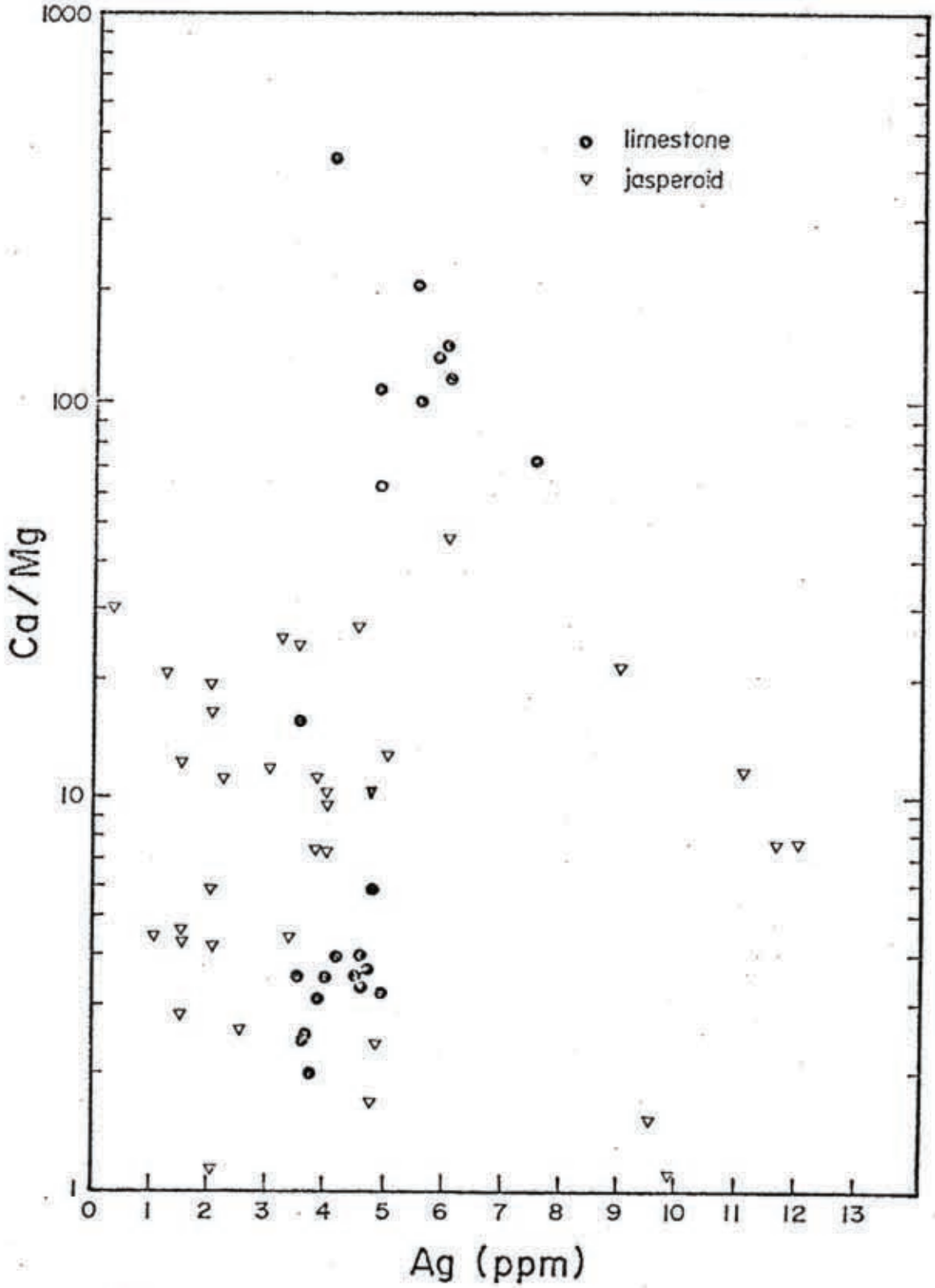

Figure 34. Graph showing relationship of calcium-magnesium ratios to silver content in limestones and jasperoids. ▾ average jasperoid concentration. o average limestone concentration.

mentioned earlier, a prospect pit on hill 10-1, which was located on jarosite alteration, was studied. One sample of jarosite (202B) and one of the iron-oxide samples were analysed chemically. There is no major change in Ag, Cu, or Pb concentrations that could be considered significant. However, there is a considerable decrease in the Ca/Mg ratio upon further weathering of the iron-oxide to jarosite.

From a few localities, samples that are rich in both barite and jasperoid, or jasperoid and crystalline quartz were analysed. These samples were separated by hand into two parts and analysed. The intent is to determine whether the Ag concentration is related to jasperoid, crystalline quartz or barite phases of deposition. Sample 5-5Qtz, 209-209Qtz and 220-220Qtz are conjugate jasperoid and crystalline quartz samples. Samples 43-43Ba and 172-172Ba are conjugate jasperoid-barite samples. It should be noted that these sample separations are not perfect but just represent biased fractions of each phase. In both cases no definitive trend is present, however Ag is present in all phases in fairly high concentrations.

Several barite rich prospect pits were also sampled and analysed. In all of these bodies the Ag, Cu, and Pb concentrations are quite high (samples 100A, 172, 230L and PP).

Finally, five analyses of the Riley-Cox Pluton were made. This was done to determine if the intrusion was enriched in Ag, Cu or Pb and could have acted as a source

for the mineralizing fluids. Turekian and Wedepohl (1961) reported the average Ag, Cu and Pb concentrations for low calcium granitic rocks as 0.037, 10 and 19 ppm respectively. The results of this study indicate that the Ag and Pb content of the Riley-Cox Pluton is higher than average.

Several characteristics of the area indicate that considerable oxidation of the jasperoid has taken place. The high relief that the jasperoid capped hills exhibit over the surrounding landscape indicates a long period of exposure. The complete transformation of essentially all the pyrite in the area to hematite, the rims of cerussite around the galena, the oxidation of some of the iron mineral to hematite and goethite, and final alteration of iron oxides to jarosite are more direct evidence of long continued oxidation and weathering of the area.

The weathering of the jasperoid in the area has greatly affected the geochemistry of the jasperoid, making interpretation difficult.

The exact nature of how the Ag, Cu, and Pb occur in the jasperoid is not known. Before oxidation they probably occurred as sulfides; the large amount of sulfur present in the jarosite and the large amount that was present in the pyrite support this. Also, the actual occurrence of galena in some of the prospect pits is more direct evidence.

Large fluctuations in the Ag, Cu and Pb assays over short distances indicate a hydrothermal type of concentra-

tion of these elements in the jasperoid. An areal plot of Ag, Cu and Pb (figures 35, 37 and 38) show no trends or concentrations, except for Ag values in the jasperoid along ridge 9-1. Figure 36 is a plot of Ag values versus distance along ridge 9-1 while going from the northwest to the southeast, beginning at sample 96. It can be seen that toward the northwest end of the ridge there is an increased content of silver. There is also a slight positive correlation of Pb and Ag along hill 9-3 but this is not thought to be significant as too few assays were used and most of the trend is due to one sample (84) of very high Pb and Ag content.

The more or less equal average concentrations of silver in the jasperoids and limestones can be explained by leaching of the jasperoid and redistribution in the limestone. The low copper concentration in the limestone with respect to the jasperoid and general lack of secondary copper mineralization (malachite) is best explained by having little copper initially present in the jasperoid.

The average Pb concentration in the limestone is higher than normal, indicating some type of post-depositional concentration. The Pb concentrations in the jasperoid are possibly close to their original value while the Pb in the limestone could be from jasperoid horizons that have now been completely eroded.

Figure 34 shows two groups of Ca/Mg ratios for the limestones, one above 70 and the other below 4. Two

Figure 35. Areal distribution of silver concentrations across the EPM mining claims. Values are given in ppm.

• Limestones

▽ Jasperoids

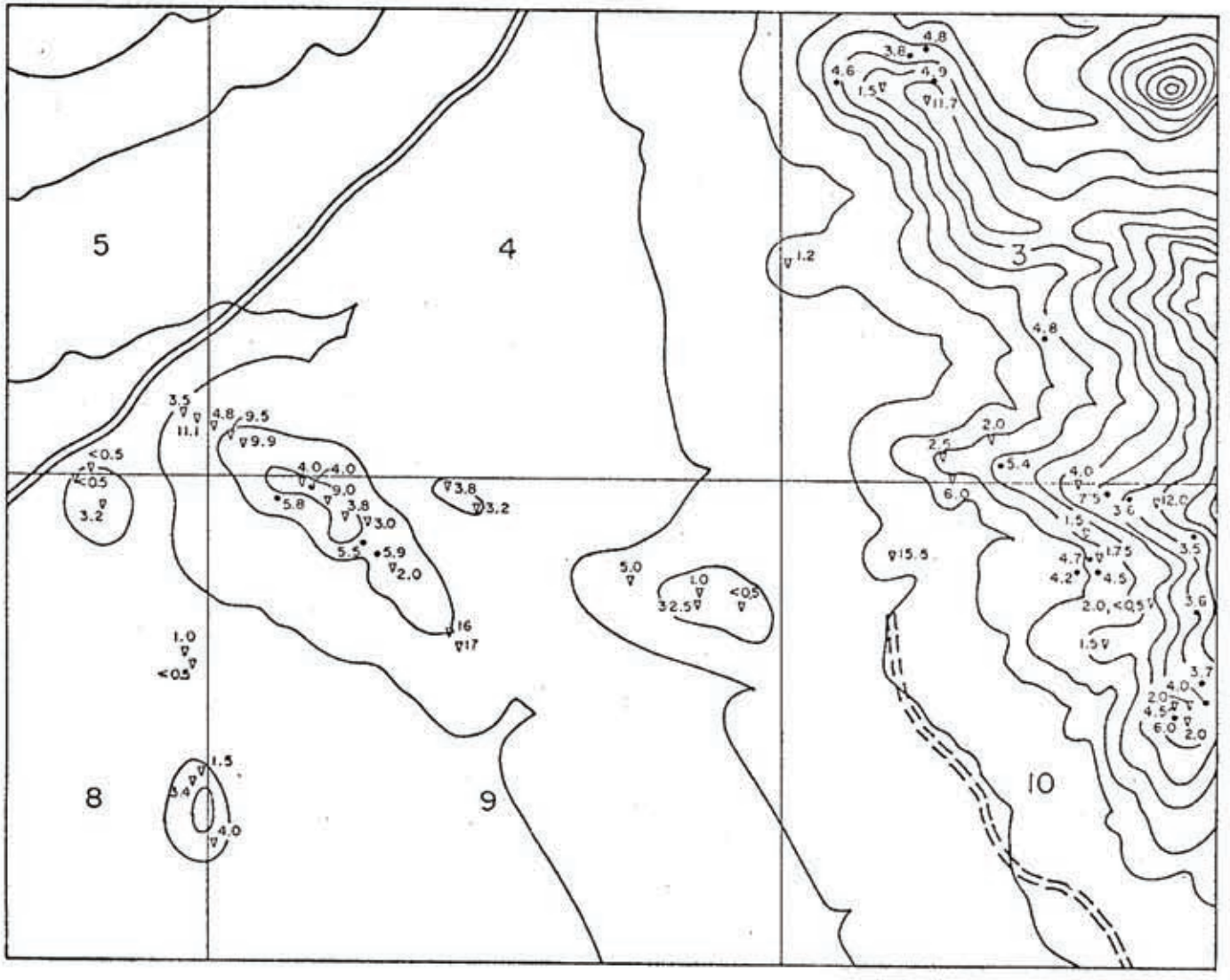
5
4
3
8
9
10
<0.5
3.2
3.5
11.1
4.8
9.5
9.9
4.0
4.0
9.0
5.8
3.8
3.0
5.5
5.9
2.0
3.8
3.2
16
17
1.0
<0.5
1.5
4.0
5.0
1.0
32.5
<0.5
1.2
4.8
2.0
2.5
5.4
4.0
6.0
7.5
3.6
12.0
1.5
15.5
4.7
1.75
3.5
4.2
4.5
2.0, <0.5
3.6
1.5
3.7
4.0
2.0
4.5
6.0
2.0

Figure 36. Graph showing decreasing trend of silver concentrations going southeast along ridge 9-1, beginning at station 96.

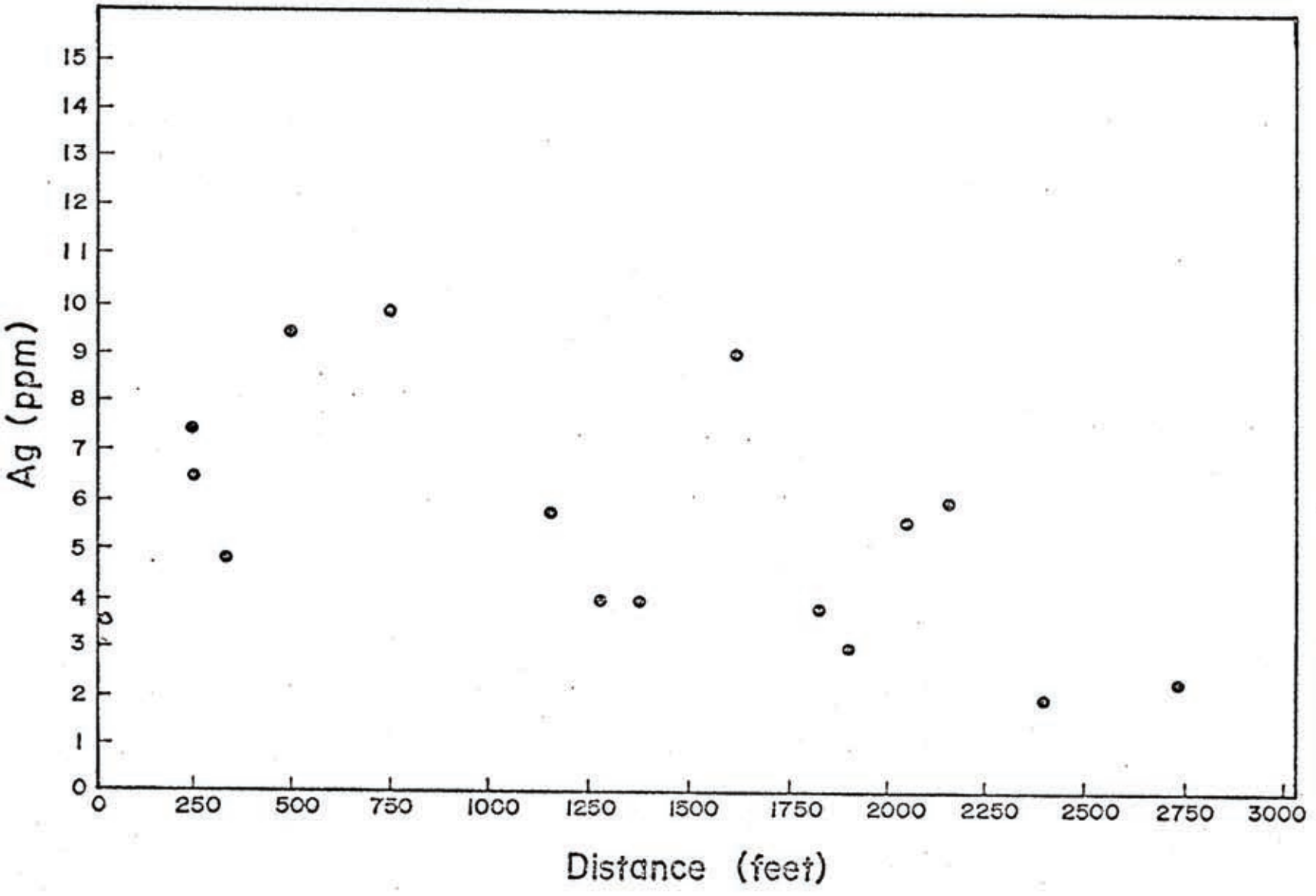
Ag (ppm)
0
1
2
3
4
5
6
7
8
9
10
11
12
13
14
15
0
250
500
750
1000
1250
1500
1750
2000
2250
2500
2750
3000
Distance (feet)

Figure 37. Areal distribution of copper concentrations across the EPM mining claims. Values are given in ppm.

• Limestones

▽ Jasperoids

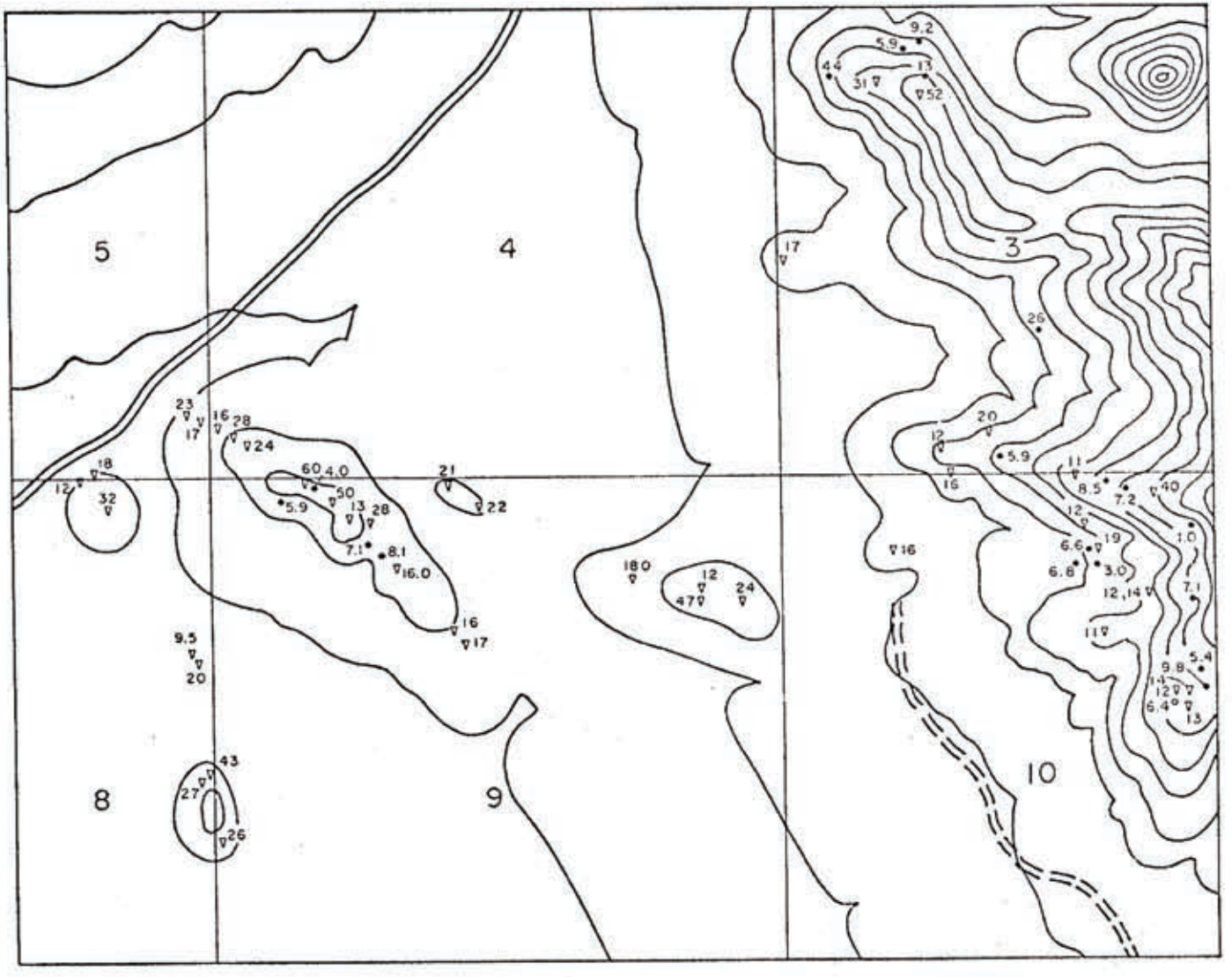
5
4
3
8
9
10
9.2
5.9
44
13
31
52
17
26
23
17
16
28
24
18
12
32
60
4.0
50
13
28
5.9
7.1
8.1
16.0
21
22
16
17
9.5
20
43
27
26
180
12
47
24
20
5.9
12
16
11
8.5
7.2
40
12
19
6.6
6.8
3.0
12,14
11
1.0
7.1
5.4
9.8
14
12
6.4
13
16

Figure 38. Areal distribution of lead concentrations across the EPM mining claims. Values are given in ppm.

• Limestones

▽ Jasperoids

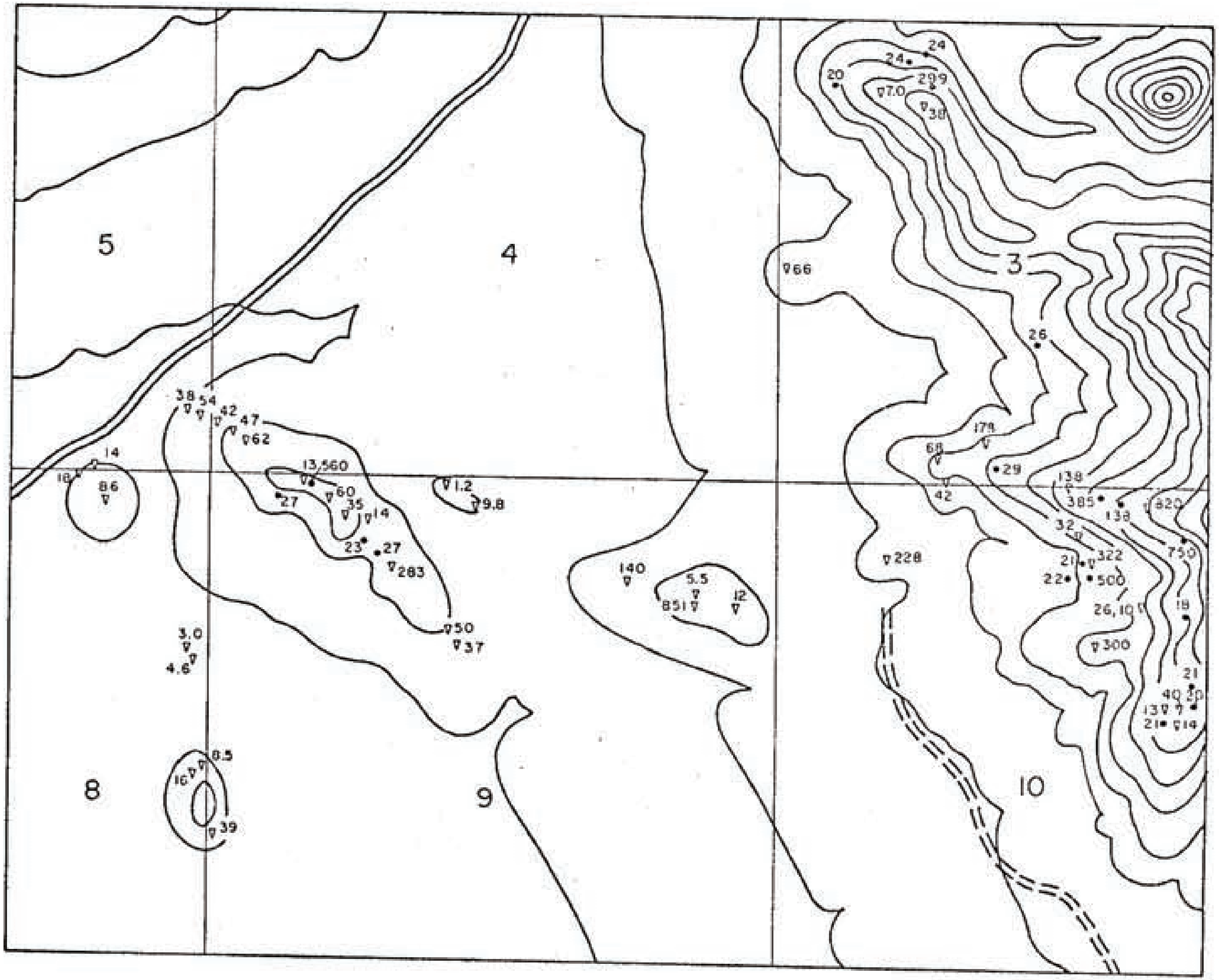
5
4
3
8
9
10
38
54
42
47
62
14
18
8.6
13,560
60
27
35
14
23
27
283
50
37
1.2
9.8
3.0
4.6
8.5
16
39
140
5.5
851
12
66
228
24
24
20
7.0
29.9
38
26
179
68
29
42
138
385
138
820
32
21
322
22
500
750
26,10
18
300
21
40
20
13
21
14

Figure 39. Areal distribution of calcium-magnesium ratios across the EPM mining claims.

• Limestones

▽ Jasperoids

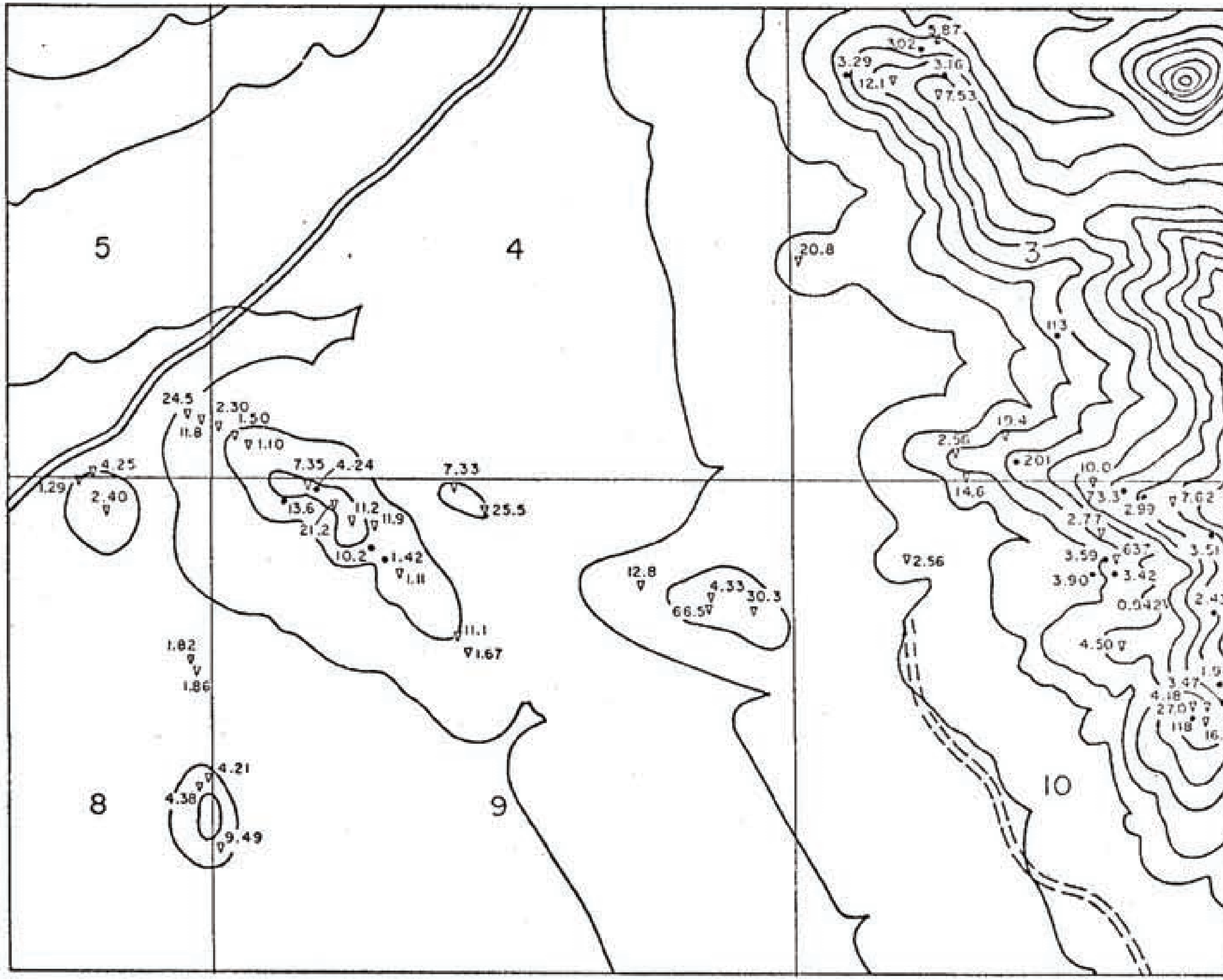
5
4
3
8
9
10
24.5
11.8
2.30
1.50
1.10
4.25
1.29
2.40
7.35
4.24
13.6
21.2
11.2
11.9
10.2
1.42
1.11
11.1
1.67
7.33
25.5
1.82
1.86
4.21
4.38
9.49
12.8
4.33
30.3
66.5
20.8
5.87
3.02
3.29
3.16
12.1
7.53
113
19.4
2.56
201
14.6
10.0
73.3
2.99
7.02
2.77
3.59
3.90
3.42
3.51
0.0421
2.43
4.50
1.94
3.47
4.18
27.0
118
16.5

possibilities are evident that could explain this; 1.) there could have been a bimodal Ca/Mg distribution in the Lueco Limestone in this area, with Ca/Mg ratios of the jasperoid fortuitously falling between these two groups, or 2.) the limestones which had Ca/Mg ratios between 4 and 20 have now been replaced by jasperoids. The fact that few limestones are found with intermediate Ca/Mg ratios and jasperoid Ca/Mg ratios are found in this region make the second explanation seem feasible. The intermediate Ca/Mg ratios of small jasperoid bodies in the northeast corner of the claims and the sharp Ca/Mg ratio changes in the jasperoid on hill 9-3, however make the first possibility seem the most likely (figure 39).

Southwest of ridge 9-1 the fossiliferous limestone bed has a high Ca/Mg ratio (greater than 70). In the east part of the area other high Ca/Mg limestone are located under jasperoid bodies. This relationship is not perfect however, as low Ca/Mg limestones are also found under jasperoid bodies and near high Ca/Mg limestones.

Geophysics

An induced polarization and resistivity survey was done across the TFT claims. A base line using 1000 foot dipoles was made along ridge 9-1 with seven lines trending NE-SW across it. A frequency domain IP was done using frequencies of 0.1 and 2.0 Hertz (Pink, 1972).

The resistivity survey indicates a high-resistivity

dike-like feature trending northwest and dipping northeast. The resistivity is the strongest under ridge 9-1. Some weak IP effects are observed in the above dike-like feature. These IP effects were not considered of economic significance by Fink (1972).

VII. Jasperoid Formation

The fact that the mineralization of the EPM claims is associated with the jasperoid, means any theory about the origin of the mineralization should account for the silicification. Lovering (1972) summarized the basic requirements needed for the formation of jasperoids:

> 1.) an adequate source of silica; 2.) fluids capable of dissolving and transporting the silica to the site of deposition; 3.) conditions at the site of deposition that caused silica to replace the host rock, and 4.) reaction rates at this site such that host rock dissolved at the same rate or a little faster than silica precipitated.

Source of Silica

The fluid inclusion data and the presence of pyrite in the jasperoid (Lovering, 1972) indicate a hydrothermal origin. It is not possible to determine conclusively what the ultimate source of the silica was; it could have originated as a residual fluid from a cooling intrusion, or from siliceous wall rocks which were leached by ascending fluids.

The close proximity of the Mt. Riley-Mt. Cox pluton to the jasperoid bodies, and its high silver and lead content make it an attractive choice as the source of the mineralizing fluids. Also, the alteration of this intrusions feldspars to kaolinite could have supplied the silica, by reactions:

1.) $2NaAlSi_3O_8 + 2H^+ + 9H_2O = H_4Al_2Si_2O_9 + 2Na^+ + 4H_4SiO_4$

2.) $2NaAlSi_3O_8 + 2H^+ + 9H_2O = H_4Al_2Si_2O_9 + 2Na^+ + 4H_4SiO_4$

The alteration of anorthite to kaolinite does not produce excess silica. The age of the Riley-Cox pluton, Tertiary, is approximately right to allow it to be the source of the silica.

Transportation and Deposition of Silica

The texture of the [illegible] jasperoids is quite similar to those of the Kelly District jasperoids in the Magdalena Mountains, Socorro Co., New Mexico. Iovenitti (1977) interpreted these textures to be the result of silica gel deposition and recrystallization. Possible desiccation cracks, spherulites and ribbon rock texture were used by Iovenitti (1977) as evidence of the silica gel origin of the jasperoid.

Deposition of the jasperoid as a silica gel is not the only mechanism that can explain the observed textures. Deposition of silica directly as microcrystalline quartz or as silica gel with essentially immediate recrystallization to microcrystalline quartz could also produce the observed textures except the ribbon rock (figure 23).

Deposition of microcrystalline quartz may be the most important mechanism in jasperoid formation. In fact, it seems to be necessary to preserve delicate original structures (fossils, bedding) that are sometimes observed in

jasperoids. This is because dehydration and recrystallization of silica gel would distort these features.

In the ERI jasperoids the only texture found indicating deposition as silica gel was ribbon rock. This texture is thought to be produced by the deposition of a silica gel which is later recrystallized to microcrystalline quartz. Recrystallization entails a volume reduction; this creates the open spaces into which the coarser quartz fraction of ribbon rock grows.

The temperature of deposition of the silica gel (jasperoid) is not known, however two lines of evidence indicate it was at a lower temperature than that of crystalline quartz. Dehler (1976) found experimentally that in the absence of algae, rapid recrystallization of silica gel to quartz begins at approximately 165°C. Fournier and Rowe (1966) believed that at depth (high temperature) the silica solubility is controlled by quartz with amorphous silica recrystallizing to the crystalline phase.

Even though ribbon rock in the ERI jasperoids indicates that some amorphous silica deposition did occur, I believe that the silica transport took place while in equilibrium with quartz.

The silica bearing solutions were most likely hot, of moderate salinity, and acidic. Fluid inclusion homogenization temperatures (Table 1) indicate high temperatures. The salinity of the solutions was discussed earlier on page 56. The alteration of the feldspars to produce the

silica points toward acid conditions as does the dissolution of the limestone to affect the replacement.

At these proposed temperatures, 185-238°C, neither salinity nor pH have an effect on silica solubility (Kennedy, 1950; and Krauskopf, 1956). This leaves essentially four mechanisms of silica deposition:

1.) change in pressure
2.) mixing with other solutions
3.) addition of CO_2
4.) drop in temperature.

A change in pressure has been shown to be an effective mechanism in the deposition of silica at very high temperatures (Kennedy, 1950). This mechanism is important only at very high (supercritical) temperatures when pressure has a large effect on fluid volume. Here temperatures of formation are subcritical and, therefore, pressure produces negligible effects on silica solubility.

Deposition of silica by mixing silica-saturated fluids with other solutions can be an important depositional mechanism. If rising hydrothermal solutions mix with cooler connate or ground water, a marked drop in temperature can be sufficient to cause supersaturation of silica (figure 40). Along with a drop in temperature, chemical changes may take place which can cause deposition, ie., large concentrations of Na^+ (Lovering and Patten, 1962). In the EPM claims this latter mechanism is probably not important since the solutions are already rich in salts. What other

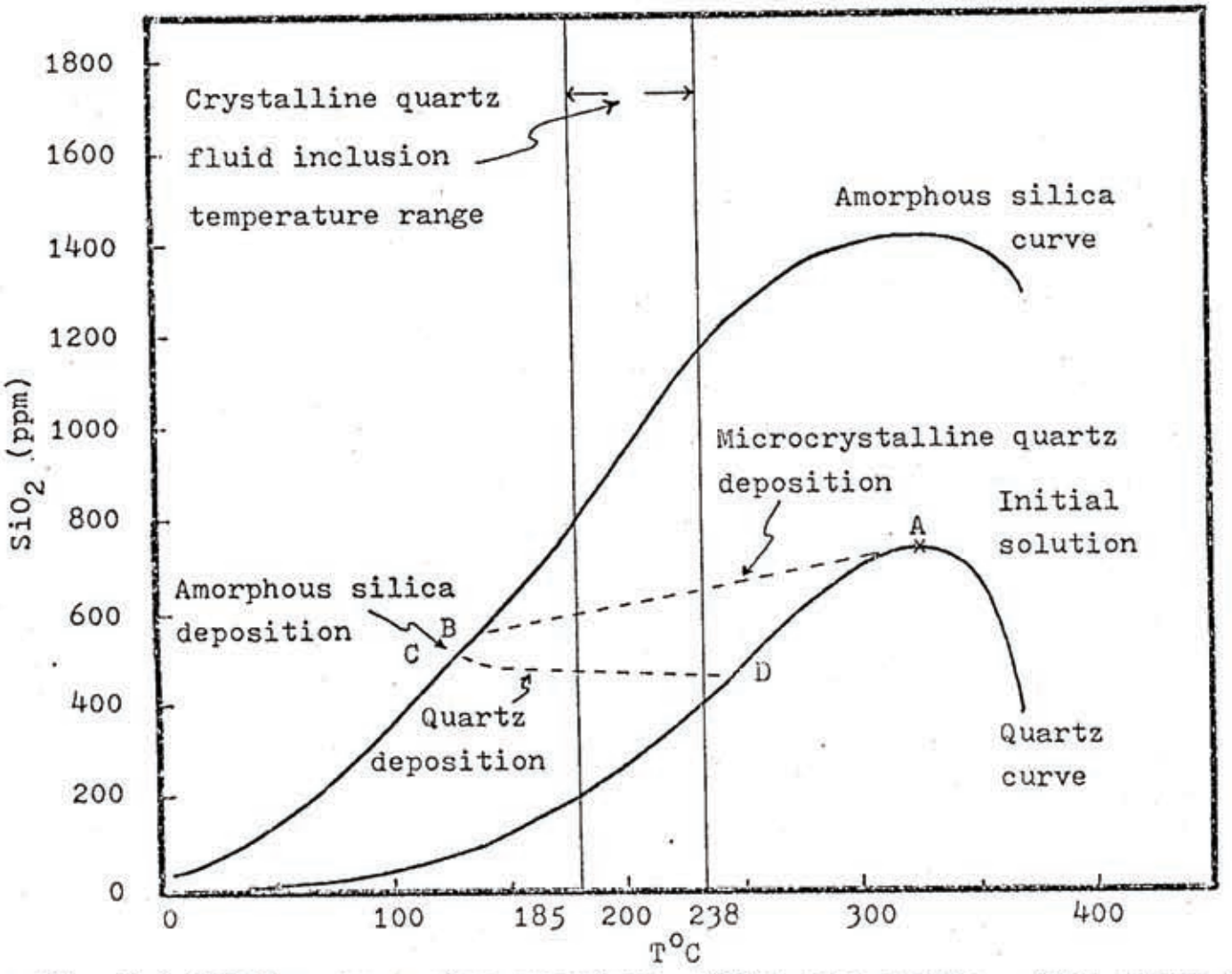

Figure 40. Solubility curves for amorphous silica and quartz. Also shown is a possible mechanism for silica deposition. Curves are after Fournier and Rowe (1966).

chemical changes and effects that may have taken place if mixing did occur cannot be evaluated specifically as no information about these solutions is available.

The strong influence that CO_2 has in deposition of silica is evidenced by the numerous jasperoid occurrences in limestones throughout the United States (Lovering, 1972). Lovering and Patten (1962) found that at 25°C in the presence of CO_2 very supersaturated solutions of silica could be caused to precipitate silica, even if limestone or dolomite were not present. They interpreted this to mean that it was the carbonic acid and not calcium bicarbonate which causes the precipitation with the presence of CO_2 apparently not changing the silica solubility but promoting flocculation of supersaturated colloidal gel.

At 185-238°C it is not likely that very supersaturated solutions of amorphous silica exist, so CO_2 is not likely to be an effective precipitating agent. Also, at the relatively low pressures and high temperatures, it is unlikely that substantial CO_2 remains in these solutions.

A drop in temperature of a saturated or nearly saturated solution is the most likely mechanism of silica supersaturation in the solutions which caused silicification of the EPM jasperoids. Fournier and Rowe (1966) summarize several studies on silica solubility. Their interpretation is shown in figure 40. This phase diagram appears to apply to these temperatures and pressures of silica deposition and recrystallization.

On figure 40 a possible mechanism for the deposition of jasperoid is shown. Initially hot, acidic solutions saturated or nearly saturated with silica in equilibrium with quartz moved up along fractures or some other channelway, as they moved up they may have mixed with other cooler solutions or passed into brecciated zones where increased surface area would cause their temperature to drop and supersaturation of quartz to occur. As these supersaturated solutions moved upward, favorable (highly permeable) limestone beds were encountered. The acidic hydrothermal solutions would tend to dissolve the limestone and the rising pH would also accelerate the precipitation of silica (Krauskopf, 1956).

Microcrystalline quartz is considered to be the first phase to precipitate out of solution. It is this variety of silica that accounts for the bulk of the jasperoid. The deposition of microcrystalline quartz takes place along the postulated curve AB; crystalline quartz does not form at this time as no open spaces are available for it to grow. When the solutions reach the amorphous silica curve (B) silica gel can be precipitated, this phenomenon takes place for only a short time producing the isolated occurrences of ribbon rock. Amorphous silica is precipitated along curve BC. With the introduction of more fluids curve CD is followed, and further replacement of limestone by microcrystalline quartz takes place. Also, crystalline quartz deposition occurs at this time. The crystalline quartz grows in

vugs, fractures and openings produced by the recrystallization of amorphous silica.

Upon reaching point D the solutions may follow the quartz solubility curve and continue to deposit quartz or more likely pass out of the system at this time.

VIII. Geologic History

The pre-Permian history of the East Potrillo Mountains is not well known as no rocks of pre-Hueco age are exposed. A thick section of pre-Hueco rocks has been postulated for the East Potrillo Mountains (Wengerd, 1969). These units are mainly limestones and dolomites, with mixed sandstones and shales (figure 10). From Cambrian through Mississippian time southwestern New Mexico was a stable shelf south of the Transcontinental arch (Corbitt and Woodard, 1973). Several periods of epeirogenic uplift are recorded by unconformities in surrounding mountain ranges.

During the Pennsylvanian and Permian approximately 3500 feet of limestones, shales, and some sandstones were deposited on the Potrillo Shelf.

Throughout the early Mesozoic, the East Potrillo Mountain area was probably a relatively stable positive area. This stability probably resulted in an erosion surface of relatively low relief on the Hueco limestone (Bowers, 1960).

During the Cretaceous, the area began to subside with sea encroachment from the south. The character of the Lower Cretaceous Noria Formation in the East Potrillo Mountains indicates near shore continental and marine deposition. Following Noria deposition, the area was uplifted and tilted slightly to the southwest, resulting in the unconformity between the Noria and the Little Horse Formation. During the period after uplift the area was again submerged and

both the Little Horse Formation and the Restless Limestone were deposited. Bowers (1960) believed that deposition probably continued into the Upper Cretaceous but subsequent erosion removed these units. Near the end of the Cretaceous tight folding and associated major thrust faulting (Laramide) of the area took place.

During the Tertiary the area was very active geologically. Unfortunately, no Tertiary rocks are now exposed to aid in interpretation. The intrusion of the Riley-Cox Pluton is considered to be one of the first events. Along with the intrusion of the pluton, andesitic and dacitic dikes were emplaced in the East Potrillo Mountains.

Following or near the end of emplacement of the Riley-Cox Pluton, the late stage high angle faulting took place. The suggested age, Eocene, (Millian, 1971) of the Riley-Cox Pluton is probably not correct but is much later. It is along these faults and fractures that the mineralizing solutions rose toward the surface, causing jasperoidization, and finally the formation of the small barite pockets. It was during this time that the East Potrillo Mountains were tilted and uplifted into their present position, by Basin and Range block faulting.

IX. Conclusions

Surface mineralization of the EPM claims is not spectacular, however subtle features point to the possibility of economic ore zones at depth.

Considering the extent of oxidation and weathering that has taken place, the silver content of the jasperoids is quite high. The high silver contents of early phases (jasperoid) and late phases (barite) indicate a long period of mineralizing fluids passing through the area which were rich in silver.

Lovering (1972) studied numerous jasperoid bodies across the United States in an attempt to determine if any characteristics are indicative of favorable jasperoid bodies (related to ore deposits). The EPM jasperoids could not be evaluated completely by Lovering's method (1972) because of a lack of analyses of some elements he studied. However some comparison was possible. Among the characteristics of the EPM jasperoids which would be considered unfavorable by Lovering's study (1972) are: color, aphanitic jigsaw-puzzle texture, late stage recrystallized calcite, and yellow-orange limonite; the presence of vugs, reticulated texture, pyrite, goethite and jarosite are considered favorable characteristics. Chemically Mg, Cu, As, Bi, Sn and Zn have concentrations which also would be considered unfavorable. Ag and Mo occur in concentrations high enough to be considered favorable. Ga and In were not analysed in

this study. From the available data, the EPM jasperoids would appear to be favorable by Lovering's (1972) study.

The proposed stratigraphic section for the East Potrillo Mountains indicates that below the Hueco Limestone there are numerous carbonate beds. These beds are likely horizons for other replacement deposits, both hypogene and supergene. Unfortunately, the drilling that has been done in the area was all shallow (less than 30 feet) and did not penetrate the zone of oxidation.

Young and Lovering (1966), Dunham (1935) and Loughlin and Koschmann (1942) describe occurrences of silicification in the Lake Valley District, Organ Mountains and Magdalena Mountains, New Mexico, respectively, which are accompanied by silver mineralization. Lovering (1972) reviews several deposits in New Mexico where silicification is present; he also gives a review of all the major mining districts in the United States where silicification is found. These papers indicate that supergene silver deposits are often found in geologic settings similar to that of the EPM claims.

Three possible ore occurrences can be envisioned to occur in the EPM claims; disseminated silver associated with the jasperoid, hypogene vein fillings and/or supergene enriched.

A disseminated silver deposit is not likely to be of any economic significance. This is based on the limited occurrence of the jasperoid and the results of the IP and resistivity surveys. The form that silver would be in in

this type of deposit is not known.

A vein filling type of deposit could be present, below the jasperoid. This type of deposit is likely to be associated with the same conduits along which the silica moved.

The most likely type of deposit that might prove to be economic is a supergene one. If a supergene deposit is present, it is likely to be very near the surface (Young and Lovering, 1966; Dunham, 1935). In this type of deposit the silver would most likely occur as cerargyrite (AgCl) because of the arid conditions that prevail in the area.

The large mass of jasperoid, the results of the IP and resistivity survey, and the increasing silver values at the northwest end of ridge 9-1 make this portion of the claims the most favorable location for further study.

X. Suggestions for Further Work

As in most cases the existence of an ore body cannot be proven until drilling has penetrated the mass. The large mass of jasperoid, and high silver values near the northwest end of ridge 9-1 indicate that this is where the most intense mineralization took place, making it the most likely spot to find ore. Any drilling program should be designed to locate either a hypogene vein filling or supergene type of deposit.

Little work can be done to further determine the location of a supergene enriched zone. To find this type of deposit straight drilling would be the most profitable method, with drilling confined to depths less than 150 feet. This type of deposit could not be located very far to the northeast of ridge 9-1 as the jasperoid dips in that direction and in a very short time becomes too deep to have been enriched by supergene processes.

In the search for hypogene vein fillings two studies may be done before drilling which may provide information that would allow better location of such deposits if they are present. A petrofabric analyses of the quartz overgrowths of the silicified quartzose siltstone might shed light on the flow direction of the silicifying solutions. Lovering (1966) found that overgrowths statistically show a maximum thickness on the stoss side of the quartz grains. A fluid inclusion study of a large number of samples across

ridge 9-1 might indicate hot spots, or areas where the mineralizing solutions were introduced. In exploration drilling for this type of deposit slant drilling northeast of ridge 9-1 toward the southwest would have the best chance of striking this type of ore body, as the body would most likely have an attitude of striking northwest and dipping very steeply.

Appendix A

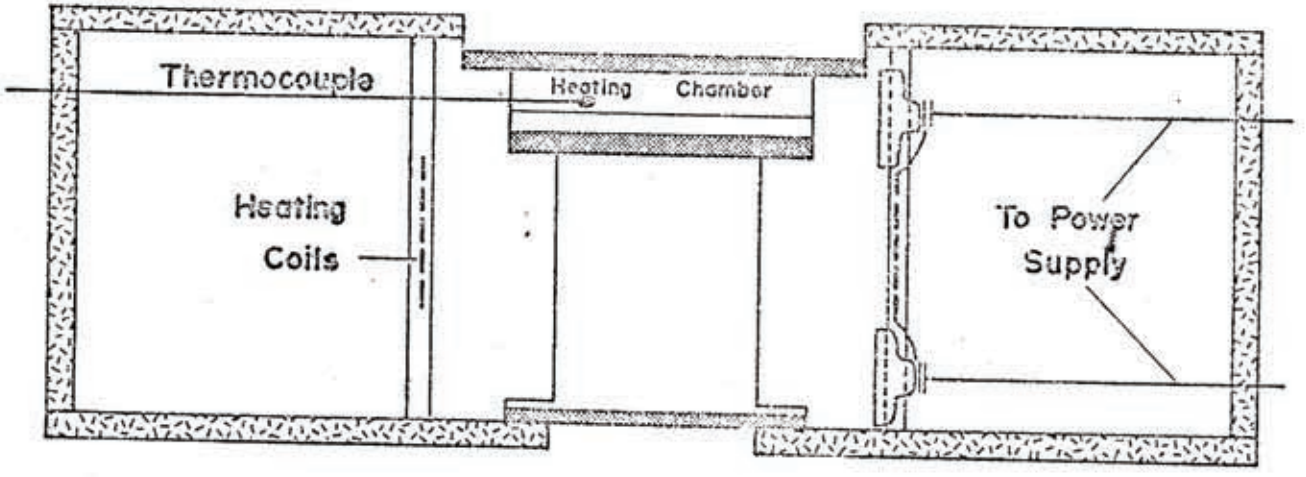

Heating Stage

aluminum

transite

pyrex glass discs

asbestos

glass wool

Specifications

Heating Coils - 1/16" x 0.0063" Nichrome V ribbon

Thermocouple - Cu-Constantine (28 gauge)

Power Supply - 0-135v, 0-5 amp, variac

Temperature Control - 0-1350° C, Sim-Ply-Trol automatic pyrometer

Appendix B

Chemical Analyses

(Run by author in NMBM laboratory)

Sample	Code	Ag (ppm)	Cu (ppm)	Pb (ppm)	Ca (%)	Mg (%)	Ca/Mg
1	(L)	4.0	4.0	560	25.4	.060	424.
5	(S)	1.0	9.5	3.0	.050	.038	1.32
5	qtz	4.2	162	38	.009	.002	4.50
10	(S)	<.5	18	14	.102	.024	4.25
43	(1)	6.5	19	2.8	.033	.017	1.94
43	(Ba)	7.5	18	16	.015	.006	2.50
70	(J)	1.0	12	5.5	.130	.030	4.33
75	(J)	4.0	26	39	.332	.035	9.49
78	(J)	1.5	43	8.5	.080	.019	4.21
79	(S)	<.5	20	4.6	.013	.007	1.86
81	(S)	3.2	32	86	.012	.005	2.40
82	(S)	<.5	12	18	.022	.017	1.29
84	(J)	32.5	47	851	.266	.004	66.5
85	(J)	<.5	24	12	.091	.003	30.3
86	(J)	5.0	180	140	.051	.004	12.8
87	(J)	3.2	22	9.8	.102	.004	25.5
88	(J)	3.8	21	1.2	.088	.012	7.33
89	(J)	2.2	16	50	.122	.011	11.1
90	(J)	2.0	16	283	.122	.110	1.11
91	(L)	5.9	8.1	27	30.2	.212	142.
92	(J)	3.0	28	14	.095	.008	11.9
93	(J)	4.0	60	13	.147	.020	7.35

Sample	Code	Ag	Cu	Pb	Ca	Mg	Ca/Mg
94	(L)	5.8	5.9	27	34.1	.250	136.
95	(J)	9.9	24	62	.078	.071	1.10
96	(J)	3.5	23	38	.098	.004	24.5
98	(J)	11.7	52	38	1.89	.251	7.53
100A	(L)	4.9	13	299	19.9	6.30	3.16
100C	(B)	6.5	22	3500	2.30	.058	39.7
110	(2)	3.4	12	61	8.00	3.25	2.46
112	(2)	5.5	60	275	2.95	.139	21.2
114	(L)	4.8	9.2	24	28.4	4.84	5.87
129	(J)	2.0	20	178	4.25	.219	19.4
130	(L)	5.4	5.9	29	30.2	.150	201
132	(J)	6.0	16	42	.540	.037	14.6
133	(3)	3.4	8.0	14	.443	.015	29.5
134	(J)	15.5	16	228	.238	.012	19.8
135	(J)	2.5	12	68	.023	.009	2.56
141	(L)	4.2	6.8	22	24.4	6.25	3.90
142	(L)	4.5	3.0	500	22.8	6.66	3.42
144	(J)	1.8	19	322	.500	.785	.637
145	(L)	4.7	6.6	21	20.4	5.68	3.59
151	(J)	<.5	12	10	.081	.086	.942
151B	(J)	2.0	14	26	.670	.117	5.73
156	(L)	3.5	9.8	380	19.8	1.27	15.6
166	(J)	4.0	11	138	5.00	.500	10.0
168	(L)	7.5	8.5	385	11.0	.150	73.3
170	(L)	3.6	7.2	138	13.9	5.58	2.49
172	(J)	12.0	40	820	.160	.021	7.62

Sample	Code	Ag	Cu	Pb	Ca	Mg	Ca/Mg
172	(Ba)	3.5	31	350	.044	.006	7.33
180	(L)	3.5	1.0	750	19.3	5.50	3.51
185	(J)	1.5	12	3.2	.166	.060	2.77
189	(L)	3.6	7.1	18	14.6	6.00	2.43
194	(6)	<.5	2.5	53	.004	.007	.571
200	(L)	3.7	5.4	21	19.4	10.0	1.94
201	(J)	2.0	14	40	.092	.022	4.18
202A	(4)	1.2	7.2	42	.013	.018	.722
202B	(5)	1.8	4.9	38	.003	.119	.025
204	(B)	0.0	22	2.5	.095	.006	15.8
205	(J)	3.4	27	16	.070	.016	4.38
207	(J)	4.8	17	37	.050	.030	1.67
208	(L)	5.5	7.1	23	26.8	.262	102
209	(J)	3.8	13	35	.067	.006	11.2
209	qtz	1.2	10	14	.009	.002	4.50
210	(J)	9.0	50	60	.510	.024	21.2
212	(J)	9.5	28	47	.012	.008	1.50
213	(J)	4.8	16	42	.184	.008	23.0
214	(J)	11.1	17	54	.189	.016	11.8
215	(J)	1.5	11	300	.027	.006	4.50
219	(L)	4.0	9.8	20	15.4	4.44	3.47
220	(J)	4.5	12	13	.135	.005	27.0
220	qtz	4.2	28	20	.010	.006	1.67
221	(L)	6.0	6.4	21	28.0	.238	118
222	(J)	2.0	13	14	.247	.015	16.5
223	(6)	3.8	12	228	8.75	.057	154

Sample	Code	Ag	Cu	Pb	Ca	Mg	Ca/Mg
225	(L)	4.6	6.2	28	23.6	6.12	3.86
230L	(B)	17.0	170	4450	.505	.023	22.0
232	(7)	2.5	9.5	26	1.46	.077	19.0
235A	(8)	3.5	8.5	1130	19.3	5.0	3.81
235B	(9)	2.5	28	400	6.55	.170	38.5
236	(L)	3.8	5.9	24	23	7.62	3.02
237	(L)	4.6	4.4	20	25.1	7.62	3.29
240	(J)	1.5	31	5.8	6.33	.051	12.4
249	(L)	4.8	26	26	27.0	.238	113.
250	(J)	1.2	17	66	.104	.005	20.8
IG-1	(10)	1.0	10	44	1.82	.272	6.69
IG-2	(10)	<.5	12	40	1.90	.675	2.81
IG-3	(10)	<.5	9.0	20	.795	.272	2.92
IG-4	(10)	<.5	12	27	1.70	.650	2.62
IG-5	(10)	1.4	14	140	2.34	.645	3.63
PP	(B)	14.5	5000	1700	8.20	.242	33.9
Glor#1	(11)	0.0	8.5	4.0	.040	.108	.370
Glor#2	(11)	0.0	9.2	3.2	.030	.065	.461

Code

(J) - Jasperoid

(B) - Barite

(L) - Limestone

(S) - Quartzose Siltstone

qtz - When following sample number it indicates that it is a sample of crystalline quartz hand picked from the

sample of the same number.

Ba - When following sample number it indicates that it is a sample of barite hand picked from the sample of the same number.

1. - made up of both jasperoid and barite
2. - made up of both limestone and jasperoid
3. - highly oxidized and weathered rock
4. - hematite and goethite
5. - jarosite, alteration of hematite, and goethite
6. - limestone and jasperoid contact
7. - sandstone of Noria Formation
8. - recrystallized limestone
9. - limestone and barite
10. - samples from Mt. Riley and Mt. Cox; IG-5 is from Mt. Riley and the rest are from Mt. Cox
11. - Glorietta sandstone, used to clean mill between sample crushings.

Appendix C

Chemical Analyses

(Run by commercial laboratory)

Sample	Ag	Cu	Pb	Ca	Mg	Zn	Mo	Ni	Co
70	1.	15	30	.5	.15	N	10	300	N
84	30.	70	3000	1.	.05	N	50	150	N
133	5.	15	100	1.	.02	N	70	70	N
134	20.	15	200	.7	.05	N	20	200	N
204	2.	50	20	.7	.03	N	N	150	N
221	L	L	10	G20	1.	N	N	L	N
230L	30	300	G10,000	1.5	.2	G10,000	300	70	N
IG-5	L	30	200	7.	2.	200	30	500	20
Detection Limit	0.5	5	10	.05	.02	200	5	5	10

Appendix C cont.

Sample	Cr	As	Sb	Mn	V	Zr	Ba	Be	Sr
70	700	N	N	100	L	N	G5000	5	500
84	500	300	N	300	L	N	GG	2	5000
133	200	GG10,000	300	50	L	N	GG	L	1500
134	700	1,000	N	70	20	200	G	L	700
204	300	N	N	15	L	N	GGGG	3	GG5000
221	70	N	N	200	70	N	3000	L	1000
230L	150	L	N	200	L	N	GGGG	L	GG
IG-5	1000	N	N	1500	100	100	3000	10	1000
Detection Limit	20	200	100	10	10	10	10	2	100

Appendix C cont.

Sample	Y	Ti	Na	K	Si	Al	P	Fe
70	N	.03	N	N	30.	1.	.1	1.
84	N	.01	N	N	30.	1.	.1	2.
133	N	.15	.5	N	30.	1.	.5	10.
134	N	.15	N	N	30.	1.	.1	2.
204	G200	.007	N	N	30.	1.	L	.5
221	N	.1	L	N	25.	2.	.1	.5
230L	N	.02	N	N	25.	1.	N	.7
IG-5	10	.3	5.	4.	30.	9.	.1	5.
Detection Limit	10	.001	.2	.5	1	.5	.1	.05

G - Greater than value shown

N - Not detected

L - Detected, but below limit of determination

Fe, Mg, Ca, Ti, Na, K, Si, Al and P reported in %, all others reported in ppm

Au, W, Cd, B, La, Bi, Sn, Sc and Nb were not detected or were below their level of detection in all samples.

Appendix D

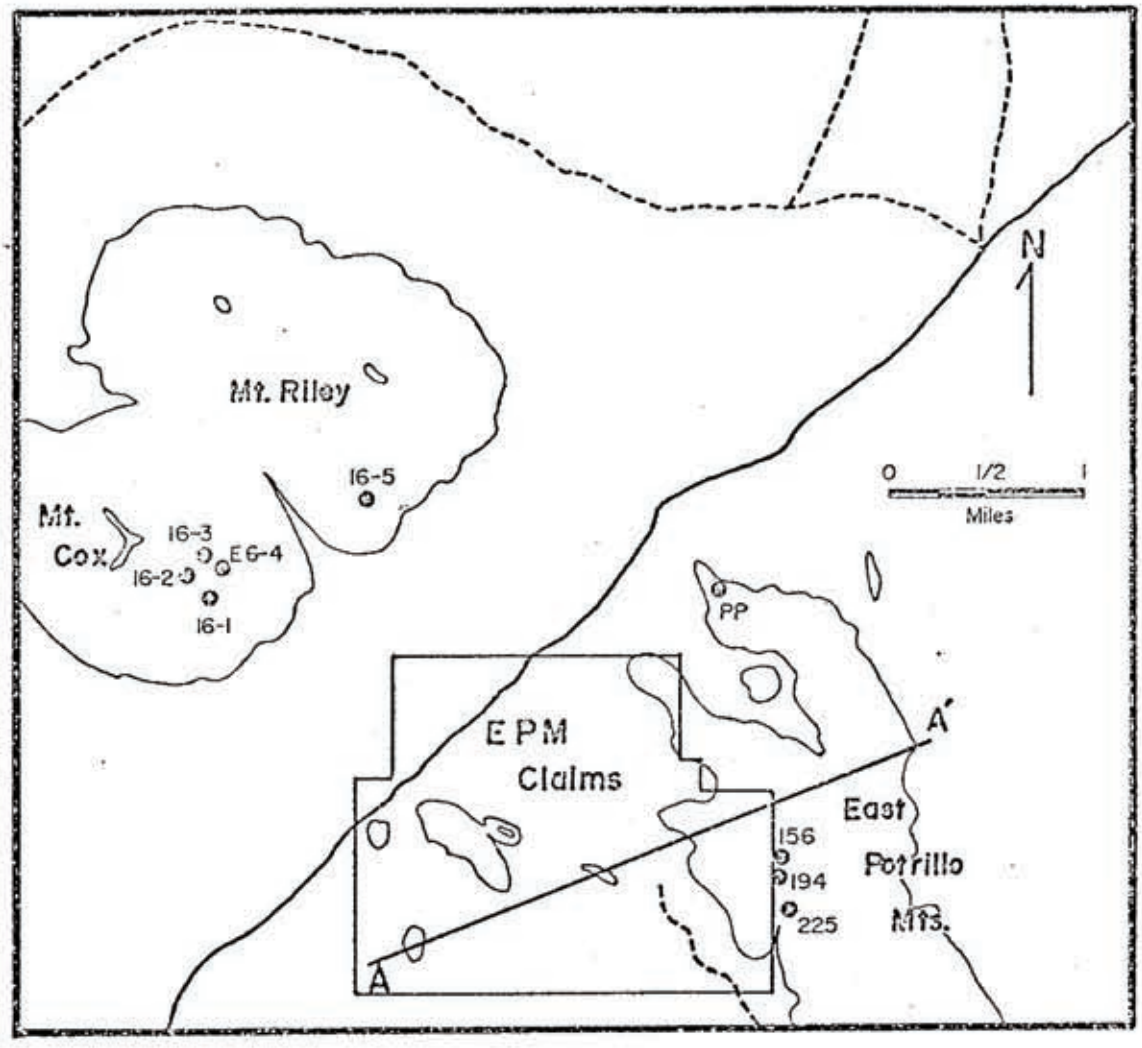

Map showing location of samples beyond the limits of the detailed map; also shown is the location of the generalized structural section.

References

Bowers, W.E., 1960, Geology of the East Potrillo Hills, Dona Ana County, New Mexico: Unpub. M.S. Thesis, University of New Mexico, 67 p.

Climatological Data, 1976, Annual Summary, New Mexico Dept. of Commerce, v. 80, n. 13.

Corbitt, L.L., 1971, Structure and stratigraphy of the Florida Mountains, Luna County, New Mexico: Unpub. Ph.D. Dissertation, University of New Mexico, 115p.

Corbitt, L.L., and Woodward, L.A., 1973, Tectonic framework of the Cordilleran foldbelt in southwestern New Mexico: Am. Assoc. of Pet. Geol. Bull., v. 57, n. 11, p. 2207-2216.

Craig, R., 1972, Stratigraphic correlation of the East Potrillo Mountains with the Sierra de Juarez: El Paso Geol. Soc. Guidebook #6, p. 17-18.

Dunham, K.C., 1935, The geology of the Organ Mountains, with an account of the geology and mineral resources of Dona Ana Co., New Mexico, N.M. Bur. of Mines Bull. 11, 272 p.

Fink, J.B., 1972, A review of induced polarization and resistivity data, EPM claims, Dona Ana County, New Mexico: Unpub. report by Phelps Dodge Corp., Tuscon, Ariz. for W.A. Bowes, Steamboat Springs, Colorado.

Folk, R.L., 1974, Petrology of Sedimentary Rocks: Hemphill Pub. Co., Austin, Texas, 182 p.

Fournier, R.O., and Rowe, J.J., 1966, Estimation of underground temperatures from the silica content of water from hot springs and wet-steam wells: Am. Jour. Sci.,

v. 264, p. 685-697.

Goldschmidt, V.M., 1954, Geochemistry: Oxford at the Clarendon Press, London, 730 p.

Hall, W.E., and Friedman, I., 1963, Composition of fluid inclusions, Cave-in-Rock fluorite district, Illinois, and Upper Mississippi Valley zinc-lead district: Econ. Geol., v. 58, n. 6, p. 886-911.

Harbour, R.L., 1972, Geology of the northern Franklin Mountains, Texas and New Mexico: U.S.G.S. Bull. 1298, 129 p.

Hawley, J.W., and Kottlowski, F.E., 1969, Quaternary geology of the south-central New Mexico border region: New Mexico Bur. of Mines Circ. 104, p. 89-115.

Hoffer, J.M., 1969, Volcanic history of the Black Mountain-Santo Tomas Basalts, Potrillo Volcanics, Dona Ana County, New Mexico: N.M. Geol. Soc. Guidebook, The Border Region, p. 108-114.

Hoffer, J.M., 1976, Geology of the Potrillo Basalt Field, south-central New Mexico: New Mexico Bur. of Mines Circ. 149, 30 p.

Hook, S., 1977, Personal Communication, New Mexico Bureau of Mines and Mineral Resources, Socorro, N.M.

Ingerson, E., 1947, Liquid inclusions in geologic thermometry: Am. Min., v. 32, p. 375-388.

Iovenitti, J., 1977, Hydrothermal silicification of the Kelly Limestone in the eastern portion of the Kelly Mining District, Socorro Co., N.M.: Differentiation of chert

from jasperoid by x-ray diffraction line profile analysis, a preliminary report: Unpub. M.S. Thesis, New Mexico Inst. of Mining and Tech., 125 p.

Kennedy, G.C., 1950, A portion of the system silica-water: Econ. Geol., v. 45, p. 629-653.

Kottlowski, F.E., 1960, Summary of Pennsylvanian sections in southwestern New Mexico and southeast Arizona: New Mexico Bur. of Mines Bull. 66, 187 p.

Kottlowski, F.E., 1963, Paleozoic and Mesozoic strata of southwestern and south-central New Mexico: New Mexico Bur. of Mines Bull. 79, 100 p.

Kottlowski, F.E., 1977, Personal Communication, New Mexico Bureau of Mines and Mineral Resources, Socorro, N.M.

Krauskopf, K.B., 1956, Dissolution and precipitation of silica at low temperatures: Geochim. et Cosmochim. Acta, v. 10, p. 1-26.

Loughlin, G.F., and Koschmann, A.H., 1942, Geology and ore deposits of the Magdalena Mining District, New Mexico: U.S.G.S. PP. 200, 168 p.

Lovering, T.S., 1966, Direction of movement of jasperoidizing solutions: U.S.G.S. Bull. 1222-F, 25 p.

Lovering, T.G., 1972, Jasperoid in the United States, its characteristics, origin, and economic significance: U.S.G.S. PP. 710, 164 p.

Lovering, T.G., and Heyl, A.V., 1974, Jasperoid as guide to mineralization in the Taylor Mining District and vicinity near Ely, Nevada: Econ. Geol., v. 69, p. 46-58.

Lovering, T.G., and Patten, L.E., 1962, The effect of CO_2 at low temperature and pressure on solutions supersaturated with silica in the presence of limestone and dolomite: Geochim. et Cosmochim. Acta, v. 26, p. 787-796.

Millican, R.S., 1971, Geology and petrography of the Tertiary Riley-Cox Pluton, Dona Ana County, New Mexico: Unpub. M.S. Thesis, University of Texas at El Paso, 87 p.

Naumov, V.N., Pachadzhanov, D.N., Kopp, A.N., and Burichenko, T.I., 1969, Behavior of copper, bismuth, silver, lead and zinc in the oxidation zone of copper-bismuth deposits of eastern Karamazar: Geochemistry Inter., v. 6, p. 1949-1054.

Oehler, J.H., 1976, Hydrothermal crystallization of silica gel: Geol. Soc. of Am. Bull., v. 87, p. 1143-1152.

Rankama, K., and Sahama, T.G., 1950, Geochemistry: University of Chicago Press, Chicago, 912 p.

Renault, J., 1970, Major-element variations in the Potrillo, Carrizozo, and McCartys Basalt Fields, New Mexico: New Mexico Bur. of Mines Circ. 113, 22 p.

Thompson, S., and Bieberman, R.A., 1975, Oil and gas exploration wells in Dona Ana County, New Mexico: New Mexico Geol. Soc. Guidebook, Las Cruces Country, p. 171-174.

Turekian, K.K., and Wedepohl, K.H., 1961, Distribution of the elements in some major units of the earths crust: Geol. Soc. of Am. Bull., v. 72, p. 175-192

U.S.D.A., 1972, Normal annual precipitation, New Mexico: Soil Conservation Service, New Mexico Water Resources,

Assessment for planning purposes, map #9.

Wengerd, S.A., 1969, Geologic history and the exploration for oil in the border region: New Mexico Geol. Soc. Guidebook, Border Region, p. 197-204.

Young, E.J., and Lovering, T.G., 1966, Jasperoids of the Lake Valley Mining District, New Mexico: U.S.G.S. Bull. 1222-D, 27 p.

Zeller, R.A., 1953, Lower Cretaceous stratigraphy of southwestern New Mexico: N.M.G.S. Fourth Field Conf., p. 142-143.

Zeller, R.A., 1965, Stratigraphy of the Big Hatchet Mountains area, New Mexico: New Mexico Bur. of Mines Mem. 16, 128 p.

This thesis is accepted on behalf of the faculty of the Institute by the following committee:

Clay T. Smith

Marc W. Bowdin

A. J. Braddock

Date Oct. 21, 1977